Calculations of Light-Matter Interactions in Dielectric Media Using Microscopic Particle-in-Cell Technique

Eric Hoogkamp

Master of Science in Physics

Ottawa-Carleton Institute of Physics

Faculty of Science

University of Ottawa

uOttawa

Acknowledgements

I would like to thank my supervisor Thomas Brabec for the opportunity to work with his group as well as the continuous support he has provided over the duration of this masters thesis project.

I am also grateful for the assistance and support in working with the MicPIC code and concepts behind it provided by my co-workers Charles Varin, Graeme Bart and Lucien Deveau.

The entire Ottawa-Carleton Institute of Physics provided an excellent framework for me to develop my skills and study in computational optics.

Computations were made on the supercomputer Briarée from Université de Montréal, managed by Calcul Québec and Compute Canada. The operation of this supercomputer is funded by the Canada Foundation for Innovation (CFI), NanoQuébec, RMGA and the Fonds de Recherche du Québec - Nature et Technologies (FRQ-NT).

My family and friends have been tremendously supportive in the years I have taken to do this work, especially my parents Brian and Lise Hoogkamp. It is their lifelong encouragement that has given me the opportunity to accomplish what I have.

Table of Contents

List of Figures

List of Tables

Abstract

The interaction between light and matter is usually modeled by approximating the material under study as a continuum. The magnitude of the material's polarization in the presence of an electric field is dependent on the atomic response via the well-known Lorentz-Lorentz relation. These continuous medium models can be used to see many light-matter effects including non-linear interactions. The goal of this thesis is to adapt and use novel computational methods to explore the microscopic origins of non-linear optical effects. The Microscopic Particle-in-Cell (MicPIC) technique, initially developed to model the laser-driven dynamics of strongly-coupled plasmas, is extended to study the non-linear scattering of light by a collection of dipoles in the atomic limit. In this thesis, we find that in one-dimensional chains of individual scatterers there are apparent boundary effects and the generation of even harmonics that do not appear in continuous media calculations. These finite structures of dipoles also exhibit a lower average response from each at odd harmonic frequencies of the driving light frequency. These results are in contradiction with the commonly used Lorentz-Lorenz relation, derived for a dipole in a 3D material with infinite volume, and suggest that MicPIC is more appropriate for calculations of nanostructures than models using the Lorentz-Lorenz relation.

1

Introduction

A simple definition of the field of optics is the study of light and how it behaves in various systems.[1] These systems may be as simple as free space allowing the electromagnetic waves to progress undisturbed; or more complex arrangements of matter with which electromagnetic radiation is scattered, reflected absorbed and re-emitted. It is through study of these light-matter interactions that incredibly powerful technologies such as radio communications, medical imaging and entire fields of study, from astronomy to particle physics, are possible.[1] The study of light-matter interactions has been a fruitful field of research and further knowledge of how these interactions occur could be quite useful.

There are various different models that can be used to study and predict the behavior of these light-matter interactions. The first model many are exposed to is geometric optics, in which light is represented as a collection of rays showing the trajectory that a concentrated packet of light would take. Geometric optics is a powerful model for macroscopic optical effects such as light reflecting off of a surface, however does not incorporate wave (phase) or interference effects.[2] The most accurate method for calculating

the evolution of light is to evaluate the electric and magnetic field values at various points distributed throughout the domain of the calculation. The finite-difference time-domain (FDTD) technique employs a regular grid of points. Time is discretized and at each of the steps in time the field values are re-evaluated according to a discretized version of Maxwell's equations (equation 1.1). The grid points can be chosen to have properties of matter where one wants to represent it in the domain, or matter can be treated entirely independently and fed into Maxwell's equations via the electric charge density (ρ) and the electric current density (J). Since the FDTD technique is a time-domain method it is capable of covering a wide range of frequencies in a single run of the calculation.[3]

$$\nabla \cdot \vec{E} = \frac{\rho}{\epsilon_0} \tag{1.1a}$$

$$\nabla \cdot \vec{B} = 0 \tag{1.1b}$$

$$\nabla \times \vec{E} = -\frac{\partial \vec{B}}{\partial t} \tag{1.1c}$$

$$\nabla \times \vec{B} = \mu_0(\vec{J} + \epsilon_0 \frac{\partial \vec{E}}{\partial t}) \tag{1.1d}$$

Many optical phenomena can be described with a high degree of accuracy using linear approximations for the light-matter interactions.[1] The assumption behind a linear approximation is that the response of a medium depends on the electric and magnetic field applied in a linear fashion. However useful the linear optical approximations can be, there are limitations, particularly when used to calculate solutions to high intensity problems. For high enough intensities the optical properties of a material may be altered by the presence a strong electric and magnetic field, which would require a non-linear model.

The cases in which non-linear optics is needed in a calculation typically require laser light to reach a high enough intensity.[4]

If a dielectric medium is exposed to an electric field $\vec{E}(t)$ then the positive charges of the atomic nuclei will be pulled along the same direction as the electric field's polarization, while the negative charges of the electrons will be pulled in the direction opposite the electric field. Macroscopically the separation of opposing charges within a medium results in a polarization $\vec{P}(t)$ which can be expressed as some medium-specific function of the applied electric field:

$$\vec{P}(t) = f(\vec{E}(t)) \tag{1.2}$$

A Taylor expansion of the dependence of polarization on the applied electric field will have a linear term followed by many non-linear terms:

$$\vec{P}(t) = \chi^{(1)}\vec{E}(t) + \chi^{(2)}|\vec{E}(t)|\vec{E}(t) + \chi^{(3)}|\vec{E}(t)|^2\vec{E}(t) + ... \tag{1.3}$$

The parameter $\chi^{(n)}$ is known as the n^{th} order electric susceptibility of the medium under study.[4] When a larger electric field is applied to a medium, higher order terms in the Taylor expansion become more relevant in the calculation of a medium's polarization response. At some point the intensity will be high enough that the contributions of higher order terms will be significant to the results, at which point the mathematics of linear optics no longer serves as a good approximation. By using higher order terms in a calculation than the linear susceptibility $\chi^{(0)}$ one starts to account for non-linear effects in light-matter interactions.[4]

If one is looking for macroscopic results that occur at scale many times larger than the light's wavelength used then a continuous medium can be used effectively. In this method a material is represented as a geometric

shape with certain optical properties such as the index of refraction, the electric and magnetic susceptibilities. These media encompass portions of the calculation domain where Maxwell's equations are integrated in order to calculate the response. Structures of continuous media can be relatively simple to construct, for example a window of length l could be entirely defined as a series of equations like equation 1.4 where P represents an array of all the optical properties important to the calculation.

$$P(x) = \begin{cases} P_{air} & x < 0 \\ P_{glass} & 0 \leq x \leq l \\ P_{air} & l < x \end{cases} \tag{1.4}$$

The continuous medium method can be used effectively for fast results of large structures. However, the microscopic scale effects of particle-particle interactions are lost. As these effects are missing in continuous media calculations, one cannot simply take the microscopic properties of individual atoms and scale them up N times, where N is the number of individual scatterers that would fit inside of a single grid unit.[2]

For studying microscopic phenomena one can approximate the medium as being a set of individual dipole scatterers that fill the medium volume, as shown in figure 1.1. This method, known as the discrete dipole approximation, can yield highly resolved results for linear problems. However as a part of the approximation, can not incorporate non-linear effects. By calculating the evolution of each dipole one can incorporate particle-particle interactions and it opens the possibility to see variance in the response at the dipole scale. With enough dipoles one can create an arbitrary domain shape, which can lead to highly accurate results if one has enough processing power for this expensive calculation.[5]

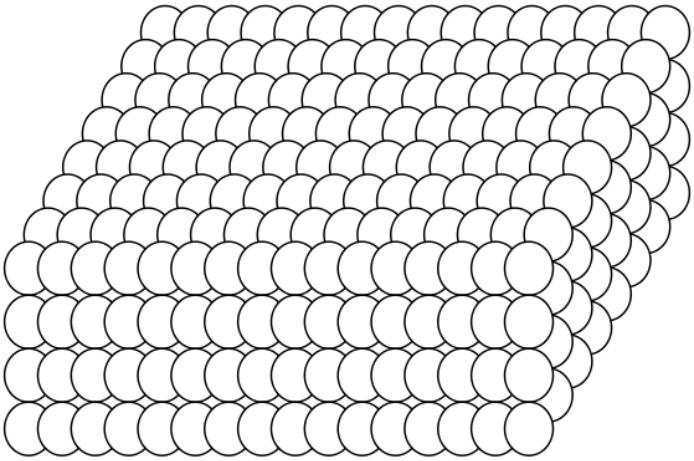

Figure 1.1: Discrete Dipole Approximation of a rectangular slab. Each sphere represents a dipole.[6]

When extending a system from one dipole to many, the electric field applied to each dipole will not be the same as that applied to an isolated dipole. In general, one has to distinguish between the macroscopic field applied by the probing light, and the effective field that each dipole experiences. The difference between the macroscopic field and the local field applied to each dipole, known as the Lorentz local field, will differ significantly unless the medium is so dilute that its linear dielectric constant is nearly 1.[4]

If one lets $\vec{E}$ be the macroscopic field and α is the linear polarizability then one can express the dipole moment in a typical dipole to be:

$$\vec{p} = \alpha \vec{E}_{loc}, \tag{1.5}$$

where $\vec{E}_{loc}$ is the local field felt by the dipole. The local field will be the combination of external sources combined with the effect of each other dipole in the medium. The local field E_{loc} will be calculated based on a procedure described by Lorentz in 1952.[4] First, one assumes that the medium has infinite volume and one can imagine a small sphere around the dipole under

study is hollowed out. The few nearby molecules that would be in this sphere are removed and would have effects that tend to cancel and so the local field at the centre will be approximately the same both with and without the surrounding sphere.[7] If one assumes that the rest of the medium has polarization $\vec{P}$ then an electrostatics calculation yields the field for a point in the center of a hollowed out sphere in an otherwise continuously polarized medium will be:[4]

$$\vec{E}_{loc} = \vec{E} + \frac{4}{3}\pi\vec{P}. \tag{1.6}$$

The definition of a material's polarization is:

$$\vec{P} = N\vec{p} \tag{1.7}$$

where N is the number density of the material. By combining the three equations 1.5 - 1.7 one finds a relation between the macroscopic field and polarization:

$$\vec{P} = N\alpha(\vec{E} + \frac{4}{3}\pi\vec{P}) \tag{1.8}$$

It is useful to express this result in the form in terms of the linear susceptibility $\chi^{(1)}$, which is done by subbing in the equation

$$\vec{P} = \chi^{(1)}\vec{E} \tag{1.9}$$

By combining equations 1.8 and 1.9 then rearranging for $\chi^{(1)}$ one finds that:

$$\chi^{(1)} = \frac{N\alpha}{1 - \frac{4}{3}\pi N\alpha}. \tag{1.10}$$

For the typical case where α is positive one can see that the susceptibility is larger than the value predicted in models that ignore local-field corrections ($N\alpha$). This result is known as the Lorentz-Lorentz relation.[4] Having a higher susceptibility will result in dipoles that will react more strongly when in a medium full of dipoles as compared to isolated ones. This is an effect that one should consider when performing continuous media calculations to account for microscopic effects.

The Microscopic Particle-in-Cell code used for this thesis is an attempt to bridge the gap between the large scale results of continuous media calculations and the labour intensive accuracy of the discrete dipole approximation while being capable of handling non-linear effects. The gap from atomic separations to visible wavelength requires that a domain must resolve at least four orders of magnitude ($\mathring{A}$ to μm) to ensure that responses at each end of these scales influence the results. There are two primarily used methods for calculating the evolution of a cluster of scatterers, known as Molecular Dynamics and the Particle-in-Cell method.[6] A combination of both methods is used for the MicPIC method adapted and applied in this thesis.

1.1 Molecular Dynamics

The Molecular Dynamics (MD) technique for calculating the evolution of a system of particles employs direct calculations of the electrostatic forces between each pair of particles. The sum of the contribution from each other particle is applied as the driving force to the particle's equations of motion, as shown in figure 1.2. By directly determining the interaction force between each pair of particles, this MD method leaves very little to approximation and is capable of obtaining highly accurate results.[8] The accuracy of this

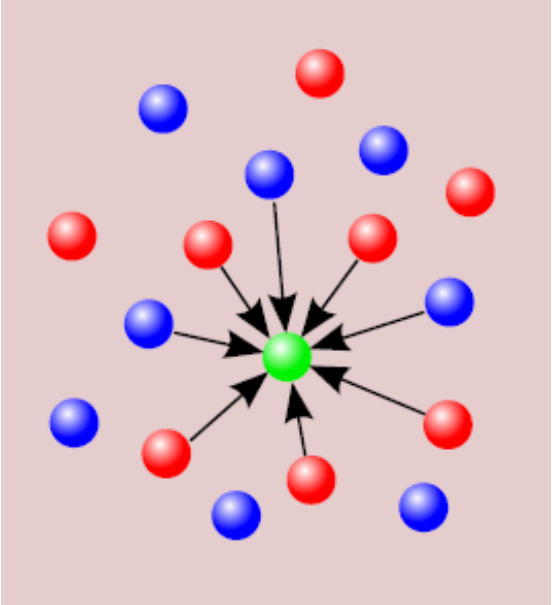

Figure 1.2: Molecular Dynamics Calculations: The effect of each blue and red particle on the current green particle is summed and used as an input to the green particle's equations of motion. This calculation is repeated for each particle in the system.[6]

MD technique comes with a few drawbacks, such as a lack of propagation effects, possible truncation errors and poor computational scaling with the size of the domain. The type of system and the results one is looking for are important factors in determining whether using an MD calculation is worth the various drawbacks.

In Molecular Dynamics calculations, the force between each particle pair is calculated directly using the Coulomb equation

$$F_C = \frac{q_1 q_2}{4\pi r^2}. \tag{1.11}$$

By accounting for particle-particle interactions in this way makes Molecular Dynamics a useful tool for electrostatic investigations at the cost of

losing any influence from propagation effects. When studying light matter interactions it is important to be capable of including the effects that external influences, such as a driving light pulse, will have on the particles. The simplest implementations of Molecular Dynamics code don't resolve propagation effects nor do they have built in means to track the electromagnetic propagation of a pulse through the medium. There are methods for adding the influence of an external electromagnetic wave to an MD system such as including a grid of field values that evolve with Maxwell's equations or having each particle calculate the electric field ($\vec{E}$) that would be applied to it by some analytic light pulse given its current position and time. Though the aforementioned methods will allow for interaction between the particles and an externally driven wave, they do not immediately allow for internal propagation effects to be studied, limiting the results that can be obtained, especially when systems with large inter-particle separations such as gases are calculated.[8]

Given a system of n particles, each one will have $n-1$ neighbours influencing it and so the calculation for the particle-particle interaction is done $n-1$ times per time step, for each particle to determine how the system will evolve. The exact force between any two particles will likely not fall on a value that can be exactly represented as a floating-point number in IEEE single precision, or even double precision. In a case where the value of the inter-particle force can not be represented exactly in memory, it is rounded to one of the nearest numbers that can be represented in such a way. This rounding error in the force is added to similar errors that appear from each other particles' contribution, which is then used in the equations of motion. A small discrepancy between where the code actually places a particle at the next time step, and where the code would have placed the particle if it were

using exact numbers will emerge. This error in the location and velocity of each particle compounds with each successive time step and has the potential to skew the results of a calculation significantly. These errors can be reduced greatly by increasing the precision of all affected numbers stored in memory, at the cost of computational speed and additional memory usage. These truncation errors are a consequence of computational techniques and one should keep them under consideration whenever performing computational calculations.[3]

The Molecular Dynamics technique does not scale well with the number of particles used. For an established system of n particles, adding the $(n+1)$th particle will require n additional calculations for the new particle's effect on the established surroundings; as well as n calculations of the system's effects on the new particle. This increase in the number of calculations to be performed is proportional to the number of particles in the system (n) and so will become more and more expensive as the system grows. The total number of calculations needed for the system will be proportional to n^2. Having an n^2 scaling means that if one increases the number of particles in the system by some multiple, the length of time required to perform all of the necessary calculations will increase by the square of that multiple applied to the system size.[3] A few methods of keeping the calculation time down are to use a small number of particles; set each calculated particle to be representative of a larger subset of the medium; or by using different techniques, such as Particle-in-Cell, to calculate the system's evolution.

1.2 Particle-in-Cell

The Particle-in-Cell (PIC) technique involves tracking the motion of individual particles within an finite-difference time-domain grid. The main difference between the PIC and Molecular Dynamics techniques is that the direct Coulomb interaction between two particles is not calculated in PIC. Instead of determining these direct particle-particle interactions some properties, such as the electric charge (ρ) and current (J) densities are extrapolated to the fixed grid points as shown in figure 1.3. The field values are then propagated through the grid using Maxwell's equations (equation: 1.1) to create a representation of the entire field over the calculation domain. When determining the force applied to a particular particle one can create an approximate value of the fields at the particle's location using a weighted average of all of the surrounding grid points.

To solve the FDTD grid one starts with Maxwell's curl equations:

$$\nabla \times \vec{E} = -\frac{\partial \vec{B}}{\partial t} \tag{1.12a}$$

$$\nabla \times \vec{B} = \mu_0(\vec{J} + \epsilon_0 \frac{\partial \vec{E}}{\partial t}) \tag{1.12b}$$

Writing out equation 1.12 in vector format yields a system of six coupled first order differential equations:[6]

$$\frac{\partial E_x}{\partial t} = \frac{1}{\epsilon_0 \mu_0}(\frac{\partial B_z}{\partial y} - \frac{\partial B_y}{\partial z}) - \frac{1}{\epsilon_0} j_x \tag{1.13a}$$

$$\frac{\partial E_y}{\partial t} = \frac{1}{\epsilon_0 \mu_0}(\frac{\partial B_x}{\partial z} - \frac{\partial B_z}{\partial x}) - \frac{1}{\epsilon_0} j_y \tag{1.13b}$$

$$\frac{\partial E_z}{\partial t} = \frac{1}{\epsilon_0 \mu_0}(\frac{\partial B_y}{\partial x} - \frac{\partial B_x}{\partial y}) - \frac{1}{\epsilon_0} j_z \tag{1.13c}$$

$$\frac{\partial B_x}{\partial t} = (\frac{\partial E_y}{\partial z} - \frac{\partial E_z}{\partial y}) \tag{1.13d}$$

$$\frac{\partial B_y}{\partial t} = (\frac{\partial E_z}{\partial x} - \frac{\partial E_x}{\partial z}) \tag{1.13e}$$

$$\frac{\partial B_z}{\partial t} = (\frac{\partial E_x}{\partial y} - \frac{\partial E_y}{\partial x}), \tag{1.13f}$$

where $\vec{E} = [E_x, E_y, E_z]$, $\vec{B} = [B_x, B_y, B_z]$ and $\vec{J} = [j_x, j_y, j_z]$. An important equation in determining the version of Maxwell's equations in an FDTD grid is the finite difference difference expression for a derivative centered about position $[x_i, y_j, z_k]$ and time t_n:[6]

$$\frac{\partial f}{\partial x} = \frac{f(x_i + \Delta x, y_j, z_k, t_n) - f(x_i - \Delta x, y_j, z_k, t_n)}{2\delta x} + \mathcal{O}(\Delta x^2), \tag{1.14}$$

where $\mathcal{O}(\Delta x^2)$ represents the second order and higher terms in the derivative and f represents any function. Applying equation 1.14 to equation 1.13a, centered around $[x_{i+1/2}, y_j, z_k]$ and dropping the $\mathcal{O}(\Delta x^2)$ term yields:

$$\frac{E_x|_{n+1/2}^{i+1/2,j,k} - E_x|_{n-1/2}^{i+1/2,j,k}}{\Delta t} = \frac{1}{\epsilon_0 \mu_0}(\frac{B_z|_n^{i+1/2,j+1/2,k} - B_z|_n^{i+1/2,j-1/2,k}}{\Delta y} - \frac{B_y|_n^{i+1/2,j,k+1/2} - B_y|_n^{i+1/2,j,k-1/2}}{\Delta z}) - \frac{1}{\epsilon_0} j_x|_n^{i+1/2,j,k}, \tag{1.15}$$

where the notation $E|_n^{i,j,k}$ shows the electric field evaluated at position $[x, y, z]$ and time n. Rearranging equation 1.15 to isolate the electric field term evaluated at $n + 1/2$ yields:

$$E_x|_{n+1/2}^{i+1/2,j,k} = E_x|_{n-1/2}^{i+1/2,j,k} + \frac{\Delta t}{\epsilon_0 \mu_0}\left(\frac{B_z|_n^{i+1/2,j+1/2,k} - B_z|_n^{i+1/2,j-1/2,k}}{\Delta y} - \frac{B_y|_n^{i+1/2,j,k+1/2} - B_y|_n^{i+1/2,j,k-1/2}}{\Delta z}\right) - \frac{\Delta t}{\epsilon_0} j_x|_n^{i+1/2,j,k} \tag{1.16}$$

This gives an explicit expression for the propagation of the electric field (E_x) and similar expressions for the other two dimensions of the electric and the magnetic field can be found similarly from equation 1.13. One may notice that the the electric and magnetic fields are never evaluated at the same time. In equation 1.16 the magnetic field is evaluated at whole integer time steps whereas the electric field is evaluated only at half integer time steps, resulting in the fields having alternating updates. The staggering of the electric and magnetic fields in space is another interesting property of equation 1.16 and to use it effectively, a simple grid with field values defined on the vertices will not work well. By altering where in the grid each field value is applied to, one can find a configuration that has exactly the terms needed to solve equation 1.16. The configuration used for the results in this thesis is staggered according to the Yee staggering.[6]

A couple of benefits to using this PIC technique are that this method will scale linearly with increasing domain size and already has an integrated method for propagation of both internal particle-particle effects and the externally driven electromagnetic field. Despite these advantages, PIC based

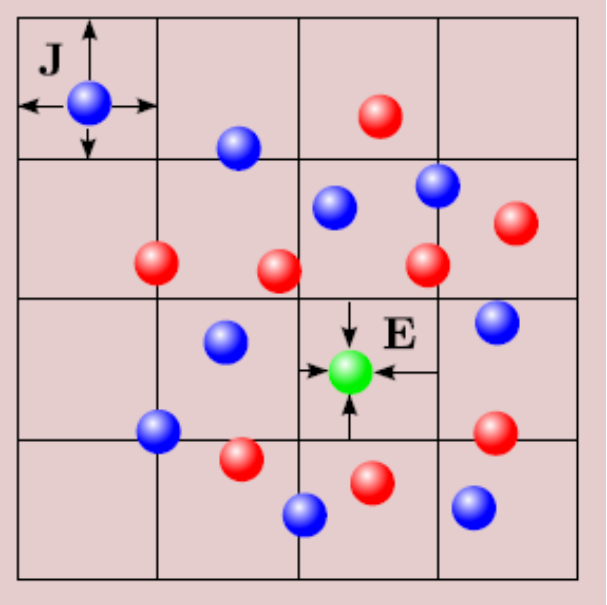

Figure 1.3: Particle-in-Cell Calculations: The density and current contributions of each particle are imposed on the surrounding mesh, which are then used to determine the field values affecting other particles.[6]

calculations are not strictly better than MD as they lose some short range accuracy of particle-particle interactions in the grid extrapolation process and the method of implementing such a code is not as intuitive compared to the MD method.[3]

Each particle in a Particle-in-Cell calculation will have a number of surrounding grid points to have its electric current and density contributions interpolated onto. For point-like particles in a three-dimensional cubic grid there will be at most 8 immediately surrounding grid points affected. The number of grid points immediately affected by a particle will be referred to as g and so for PIC calculations for point-like particles one has $g = 8$. Using only the closest grid values the shape of a particle effectively takes the shape of a single grid unit, losing the spherical symmetry of a charged particle's

influence on its surroundings. One method for reducing the loss in spherical symmetry is to have each particle's effect on the grid spread beyond the very closets grid points. Spreading a particle's charge over a Gaussian distribution centered at the discrete particle's position helps to smooth out the forces at the cost of increasing the value g, adding to the computational time for each particle's influence on the system. The total number of calculations added by introducing one new particle will only depend on this constant value g, since each particle's entire interaction with the system is determined through its closest surround grid points. As this increase in the number of calculations is entirely independent of the current number of particles in the system n, the calculation length will scale linearly with n, giving a much better scaling than the n^2 scaling of the Molecular Dynamics method.[3] In addition to adding particles, one can extend the domain size of a PIC calculation and increase the computation time. Unlike in Molecular Dynamics codes, where a grid is not used and the particles can be added anywhere for the same computational cost, adding a particle outside of a PIC code's domain will require an extension of the FDTD grid to contain the new particle. Each grid point updates once per time step based on a constant number of surrounding grid points and the relatively constant number of nearby particles, resulting in another linear scaling.

When a pair of charged particles come close to one another the Coulomb interaction between them will grow based on the $1/|r^2|$ (equation 1.11) dependence of the electrostatic force. When one particle's influence on the system is interpolated onto its surrounding grid points and then applied to the other nearby particle, the fact that these two particles are very close to one another is partially lost. The two particles' influences on one another will not be calculated in accordance with the electrostatic Coulomb equa-

tion, especially if they are within the same grid unit. The force calculated through the grid-particle interactions can be weaker than the more direct MD calculation as the appropriate grid points likely do not lie in a perfectly straight line between the two particles, making the effective distance between a pair of particles grow based on positions relative to the grid. The forces between the two particles will be less than the electrostatic equivalent due to the $1/|r^2|$ dependence of electric forces. This short range error can be overcome by ensuring that there are plenty of grid points in between each pair of particles or by dealing with short range forces in a different way. Correcting for this poor short range force calculation is a key feature of the Microscopic Particle-in-Cell method.[6]

1.3 Microscopic Particle-in-Cell

The technique used for the majority of the results presented in this thesis combines both the short range accuracy of Molecular Dynamics with the efficient scaling and long range propagation of the Particle-in-Cell method. This hybrid combination of methods is called the Microscopic Particle-in-Cell (MicPIC)[6] technique and a visual representation of this mechanism for particle interactions is displayed in figure 1.4. Similar to the PIC method, each particle's motion will influence the electric charge (ρ) and current ($\vec{J}$) densities which are applied to the surrounding FDTD grid and fed into Maxwell's equations.[6] Maxwell's equations are solved on the grid allowing the field to propagate through the calculation domain and in turn influence the other particles. When a pair of particles are separated by less than some short distance threshold, the MD technique is used to determine the direct effect of these two particles on one another and applies it directly instead of using

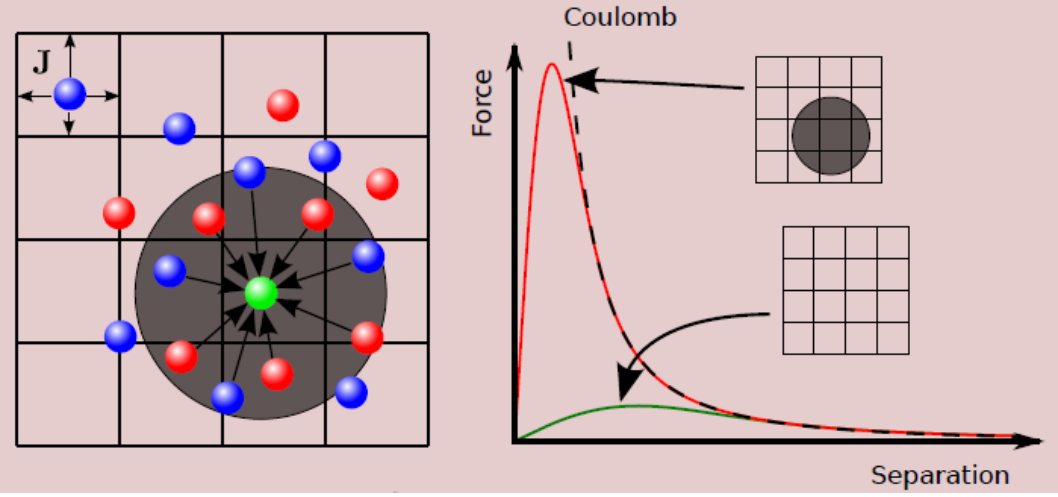

Figure 1.4: MicPIC PIC Comparison: The accuracy of Particle-in-Cell techniques is worst for the forces experienced between near-neighbouring particles (green curve). When a more direct calculation of Molecular Dynamics is used for these short range particle-particle interactions the resulting force is much closer (red curve) to the expected Coulomb force (dotted curve).[6]

the less accurate PIC technique.[6] By using this MicPIC technique to solve a system of particles the resulting accuracy is better than PIC when the system involves close range particles, and more accurate than MD for scales large enough propagation effects to occur. Accuracy is not the only quality of MicPIC, it also has better computational scaling than MD, a built in framework for field propagation and the flexibility to be applicable in many situations. By choosing an appropriate threshold value for the direct particle-particle interactions, the MicPIC code is able to be tuned to the scaling and accuracy needed in between those of the two underlying techniques.[6] It is for these reasons that MicPIC is a powerful coding technique for studying non-linear optics in the atomic limit.

With the hybrid MicPIC technique a desired level of accuracy can be

achieved with a combination of the linear PIC scaling and a small fraction of the n^2 scaling from MD. The applied threshold distance at which these two calculation techniques are separated is an important variable in determining the extent of the trade off between accuracy and speed. One can imagine that in the two extreme cases the MicPIC technique reduces to one of the two underlying techniques. If the threshold distance is large enough that each particle pair falls within that range then each particle-particle interaction is being calculated electro-statically and any propagation dependence of these interactions is lost, leaving the MD technique with a grid for the external field influences. Similarly if the threshold distance is so low that no two particles are within that range of one another then each particle's interaction will be resolved using the interpolated grid values and their evolution, leaving the PIC technique.

As the hybrid technique will approach MD and PIC in different extremes one would expect that the scaling of such a problem will also converge to that of the original techniques in these limits. Adding one particle to an established system will increase the calculation number by a constant amount $2g$ based on the Particle-in-Cell component where g represents the number of grid points that are immediately affect or are affected by a newly added particle. There is also an increase of $2NV$ calculations due to the MD part of the technique, where N is the particle density and V represents the volume enclosed by a sphere with radius equal to the threshold distance, making $2NV$ equal to twice the number of nearby particles that are close enough for the short range MD calculation. If in scaling the system up the particles are all added in the same area this calculation will scale as n^2 but that is not typically how systems are scaled to higher particle counts. If instead the new particles are distributed evenly throughout the system the scaling will fall

somewhere between linear and quadratic with particle number, depending on the threshold distance applied. By ensuring that an appropriate value is chosen for the threshold distance between MD and PIC calculations one can tune MicPIC to the level of accuracy or scaling needed for the calculation at hand.[6]

One issue that comes up with both the Particle-in-Cell method and MicPIC is the generation of what's known as a self force. If a particle's field and current contributions are imposed on a surrounding grid, along with the contributions of many other particles, and then those values are used to apply a force on the initial particle it will feel a force that has been generated by itself.[6] The self force must be removed when the grid's effect on a particle is determined or there will be an additional repulsion of each particle from the closest grid points which is non-physical behavior. In MicPIC the issues that arise from the self force effect can be more prevalent than they are in the PIC technique. For a pair of particles that are within the MD threshold distance of one another each will apply current and charge densities to the grid through PIC and the particles will influence each other directly through MD. So for particle pairs that are close together their influence on one another is applied twice. MicPIC is equipped with methods of removing the field influences for dipoles interacting electrostatically.[6]

2

Dielectric Adaptation

The majority of the results to be presented are products of an adaptation to the MicPIC code created for this thesis. The new version introduces bound electron and ion pairs as well as the equations of motion to have these pairs act as a classical dipole in MicPIC. With dipoles available one can use the MicPIC technique to calculate interactions between light and dielectric media. Using classical dipoles is applicable for systems with a low enough energy to have electrons stay in a state bound to their host ion, as opposed to the high energy plasma calculations MicPIC has been used for in the past.[9]

2.1 Bound Electrons as Oscillating Dipoles

The implementation for modeling low energy dielectrics starts with two independent charged particles, the electron and the ion. The electron has charge $-e$ as expected, however its charge is not entirely confined to one point, it is represented as a Gaussian distribution of the charge spread over several unit grid lengths when interacting with the PIC grid. The spreading of the particles allows for MicPIC to conserve their spherical symmetry better in

the cubic FDTD grid. The electrons are bound to ions which are computationally built similar to the electron, however they are much more massive and carry charge $(Z - N_e) * e$, where Z is its atomic number, N_e represents the number of electrons that are bound to the ion in lower orbitals that are not to be included in the calculation. When bound an electron will tend to stay close to its host ion and so the effect of this particle pair on the rest of the system can be closely represented by a dipole, much like in figure 2.1. To have the electron-ion pair acting like a bound system they must be made to follow appropriate equations of motion. The method of modeling a bound electron-ion pair used in this thesis is to treat the system as a Lorentz Oscillator and ensure that it evolves according to equation 2.1.

$$\vec{a} + 2\gamma\vec{v} + \omega^2\vec{x} - \sigma|\vec{x}|^2\vec{x} = \frac{q}{m}\vec{E} \tag{2.1}$$

Here m is the particle cloud's mass, γ is a decay constant for the bound pair's oscillation, ω is the resonant frequency for the dipole's binding, σ represents the strength of the third order response of the dipole, $\vec{E}$ is the electric field felt by the electron from all sources in the system other than its parent ion and $\vec{x}$, $\vec{v}$, $\vec{a}$ represent the position, velocity and acceleration of the bound electron with respect to its parent ion. The restoring force acts in a similar fashion to a simple spring system with constant $k = m\omega^2$, damping proportional to γ and a driving force that comes from the external electric field.[4]

The Lorentz Oscillator equation (equation: 2.1) is a second order differential equation in time, so in order to more easily implement it in to the MicPIC code it will be reduced to a pair of first order differential equations.[3] The leapfrog technique used in MicPIC's FDTD solver involves calculating the velocity and position of the particles under study at alternating time steps. The leapfrog method allows for a system of two first order differential equations to

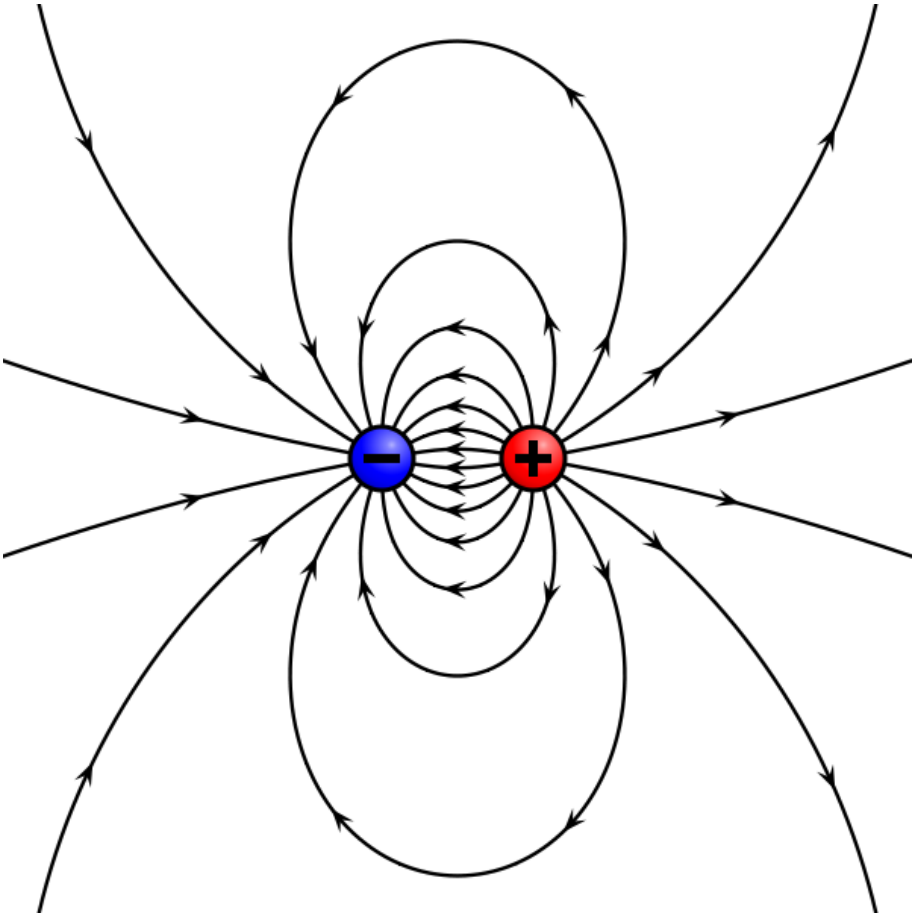

Figure 2.1: Depiction of a Dipole: When the positive charge (ion) and the negative charge (electron) are relatively close together the generated electric field approaches that of one where the charges are separated by an infinitesimal distance, which is a dipole.[6]

replace the more difficult to integrate second order differential equation 2.1.[6] The first of these equations is derived from rearranging the discrete definition of average velocity with $dx = x^{(n+1)} - x^{(n)}$ and $dt = t^{(n+1)} - t^{(n)} = \Delta t$ and centering the derivative around n, as shown in equation 2.2.

$$\begin{gathered} \vec{v} = \frac{d\vec{x}}{dt} \\ \Rightarrow \vec{x}^{(n+1)} = \vec{x}^{(n)} + \Delta t \vec{v}^{(n+1/2)} \end{gathered} \tag{2.2}$$

The derivation of the second equation begins similarly to the first, starting with the definition for acceleration instead of velocity as seen in equation 2.3. The acceleration term is where the the bound motion of the particles is applied by subbing in equation 2.1. The application of the Lorentz Oscillator's acceleration allows the particle pair to be influenced by their separation x, relative velocity v and external electric fields E. The two equations 2.2 and 2.3 have been carefully manipulated to ensure that position values are only needed and calculated on whole integer time step intervals, while velocities only appear on half integer time steps. The method of calculating velocity and position one after another at alternating time steps is intentional to ensure that the dipole equations fit well with the FDTD technique used for field propagation in MicPIC.[6]

$$\begin{gathered} \vec{a} = \frac{d\vec{v}}{dt} \\ \Rightarrow \vec{v}^{(n+1/2)} = \vec{v}^{(n-1/2)} + \Delta t \vec{a}^{(n)} \\ \Rightarrow \vec{v}^{(n+1/2)} = \vec{v}^{(n-1/2)} + \Delta t(-2\gamma \frac{\vec{v}^{(n+1/2)} + \vec{v}^{(n-1/2)}}{2} - \omega^2 \vec{x}^{(n)} + \sigma |\vec{x}|^2 \vec{x} + \frac{q}{m} \vec{E}^{(n)}) \\ \Rightarrow \vec{v}^{(n+1/2)} = \frac{1}{1 + \Delta t \gamma} (\vec{v}^{(n-1/2)} + \Delta t(-\gamma \vec{v}^{(n-1/2)} - \omega^2 \vec{x}^{(n)} + \sigma |\vec{x}|^2 \vec{x} + \frac{q}{m} \vec{E}^{(n)})) \end{gathered} \tag{2.3}$$

With equations 2.2 and 2.3 one can have an electron-ion pair following the Lorentz equation 2.1 within an FDTD grid. Having these equations is a start to adapting MicPIC to be capable of handling low energy dielectric calculations, however without any other changes MicPIC would account for the interaction between an electron and its host ion twice. Their interaction is calculated once through the leapfrog algorithm developed, and once through the electrostatic Molecular Dynamics calculation applied to any close particle pairs in MicPIC. The field effects of the electron on its host ion and vice versa has to be removed. This is done by switching off direct forces created between the electron and ion in each individual dipole.

To remedy this doubling of the electron-ion influence, the direct MD calculation between the bound particles is removed without disrupting the removal of the third force that is calculated between the two from the PIC grid. One can produce physical results of dielectric media with MicPIC only by ensuring that the correct one of these three independent forces is applied between bound pairs, close but unbound pairs and distant unbound pairs of particles. These forces are determined by carefully tracking which forces are counted in which interactions.

2.2 Verification

Before any results can be confidently presented the adaptation to MicPIC must be used to recreate results that are known to be correct. The first test of the oscillating dipole system is to compare the motion profile of an individual dipole against the known solution to the classical harmonic oscillator.[1] To make this comparison, the third order term of the dipole's restoring force is ignored, no external field is applied to the dipole and the bound electron is

given an initial non-zero velocity which is allowed to evolve according to the dipole's equations of motion. Various time step durations are used to show in figure 2.2 that as a finer step size is used the output of MicPIC converges to the expected analytic result.

The test shown in figure 2.2 indicates that the implementation of the first order restoring force fits well with the analytically expected results, provided a small enough time step is used. The next term in the introduced dipole equation of motion to check is the decay term. If a dipole has some amount of energy the decay term will govern how quickly this energy is radiated away. A damped harmonic oscillator can have its damping characterized in three different types: over damping, under damping and critical damping. These classes of damping for a single, isolated dipole are displayed in figure 2.3.

Figure 2.3 shows that the damping term is functional and is capable of replicating all three types of damping. The final parameter in the dipole motion equation to validate is the third order correction term. The effect of the third order term is dependent on the separation of the electron and its host cubed ($|\vec{x}|^3$). For the oscillator model implemented the third order contribution acts as a repelling force. At great distances the first order restoring force becomes stronger between the ion and electron, which is not how this force would evolve for unbound pairs. The third order repulsive force helps to smooth out the transition between the $|\vec{x}|$ dependence of the binding force and the $1/|\vec{x}|^2$ dependence of free pairs of charged particles. While the inclusion of this third order response may result in a more accurate approximation to real particle-particle interactions it does introduce a potential instability for high energy electrons. If the distance between the electron and its host ion increases to the point where the third order repulsive force is stronger than the restoring force then the electron will continue to move farther and

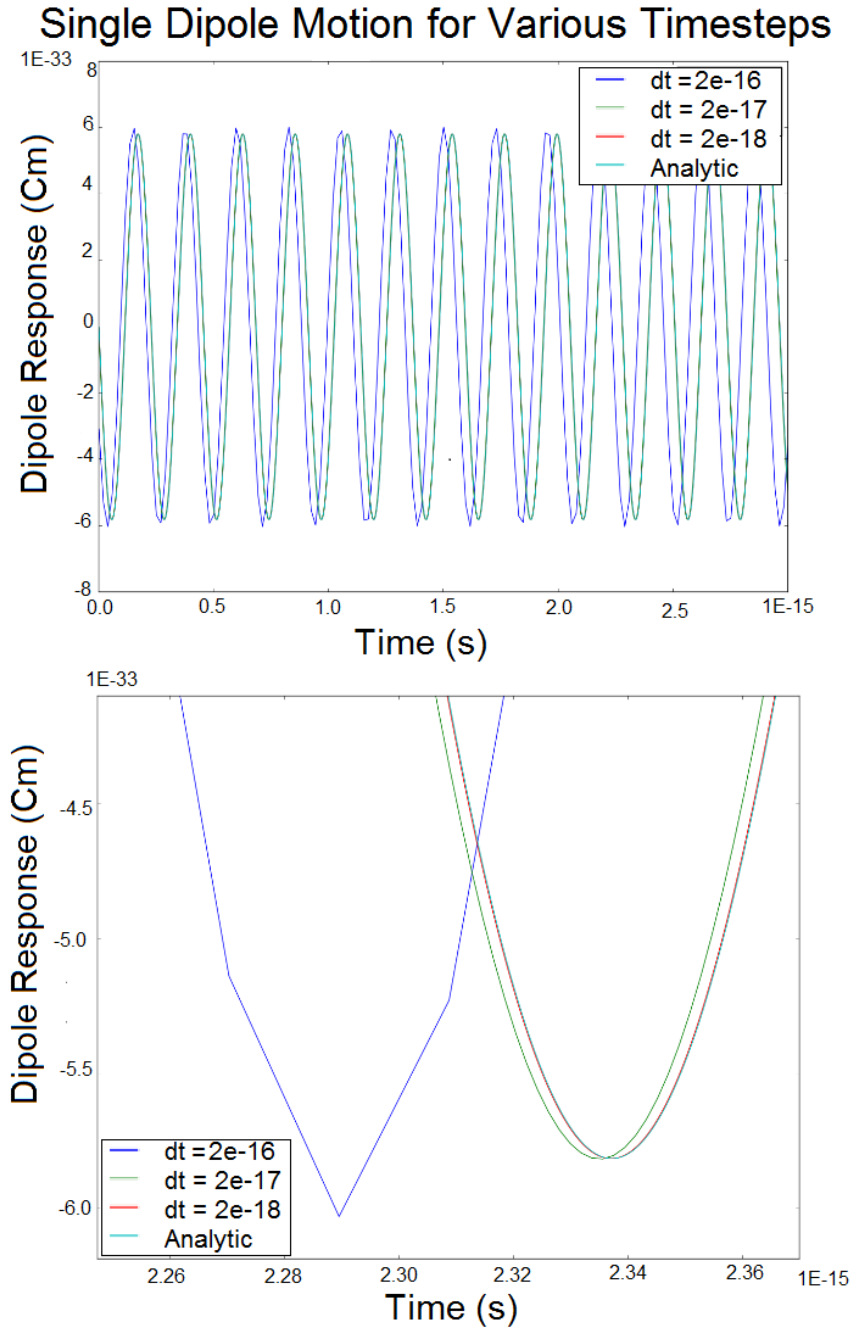

Figure 2.2: Graphical representation of the dipole moment evolution using various time steps and comparing them to the expected analytic response with a macroscopic scale (top) and a microscopic scale (bottom).[10]

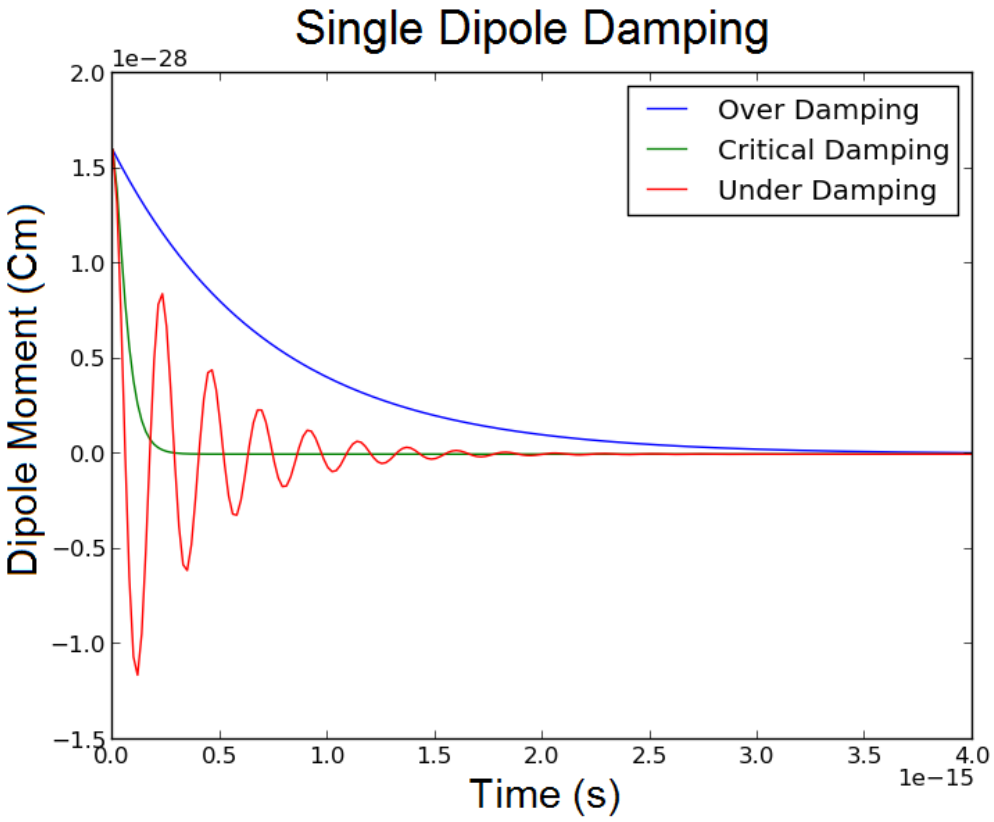

Figure 2.3: Graphical representation of the dipole moment evolution using different damping constants to show over, critical and under damping.[10]

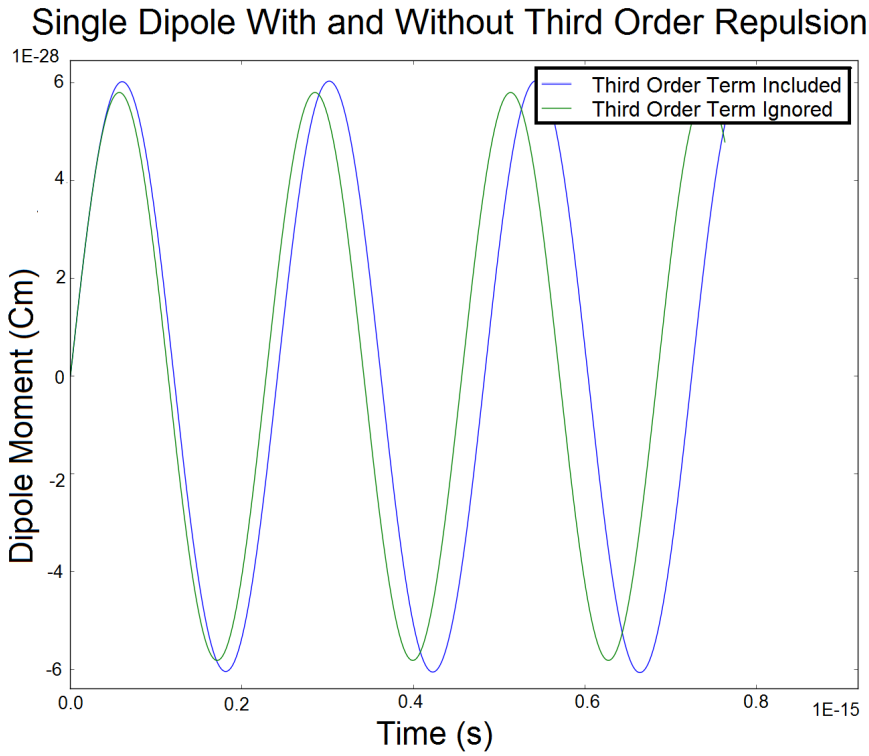

Figure 2.4: Graphical representation of the dipole moment evolution of a bound pair with and without the third order repulsion term.[10]

farther away from its host until it leaves the calculation domain. This instability is avoided by ensuring that the energies used to obtain results are low enough that the restoring force is always stronger than the repulsion. Future work with the MicPIC code will include ionization routines to ensure that this instability does not occur. The effect of this third order term is shown in figure 2.4.

Here the addition of a repulsion between the ion and electron increases the magnitude of the dipole response and decreases the frequency at which the dipole oscillates. The effect of introducing a third order term to a dipole's

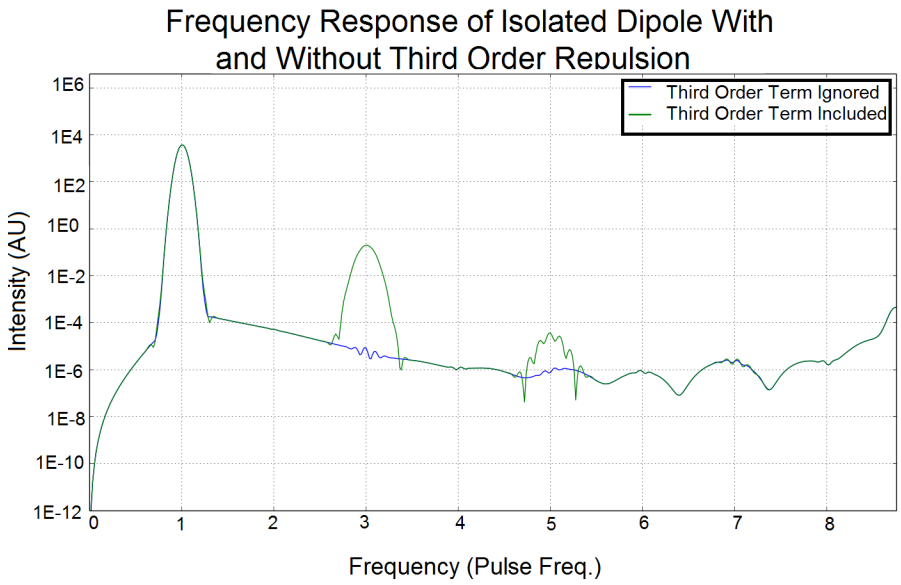

Figure 2.5: Graphical representation of the dipole moment's evolution of an isolated dipole with and without the third order repulsion term as a light pulse passes through the system. The graph is displayed in the frequency domain to clearly show the influence at thrice the incoming light pulse's frequency.[10]

response is observed when a dipole with and a dipole without the third order term included are both excited by a light pulse and displayed in figure 2.5. One can easily see the difference at 3 and 5 times the light's driving frequency between the two dipoles created by the third order term.

With each of the terms introduced in the classical dipole equations of motion working as expected in MicPIC one can move on to results of these dipoles when used to calculate responses of dielectric media.

3

Analysis

With the dielectric adaptation of MicPIC giving expected results for isolated scatterers it is time to explore more complex systems to see how these scatterers will interact with one another in the presence of light. When determining how to set up the system there are many parameters in MicPIC that need to be considered to ensure that the system one wants to describe is closely reflected by the calculation domain. Some of the first parameters to consider are values related to the descriptions of the individual particles, such as their charge, weight, size and the values of the parameters in their equations of motion, whose values were chosen based on the properties of nitrogen.[4] Once the internal workings of individual particles are decided, properties of the structure of particles can be determined, such as its size, density and the initial energy of the medium. There are also parameters relating to any electromagnetic field that will be applied, such as its intensity, frequency and pulse width. There are also internal values for the calculations, such as the threshold distance for the MD to PIC cutoff, time-step, grid size and total calculation time. The values for these parameters will be equal to those found in table 3.1 unless otherwise specified for the results in this thesis.

Table 3.1: Various default MicPIC parameters.[4][6][11]

Parameter	Value Unless Otherwise Stated
Dipole Restoring Frequency ω	$2.0662038183 * 10^{16}$ rad/s
Dipole Decay Constant γ	$2.0662038183 * 10^{14}$ rad/s
Dipole Third Order Term σ	$1.5255571 * 10^{56}$ (m s)$^{-2}$
Electron Charge e	$-1.602 * 10^{-19}$ C
Ion Charge $-e$	$1.602 * 10^{-19}$ C
Electron Mass m	$-9.109 * 10^{-31}$ kg
Ion Mass m	$2.325 * 10^{-26}$ kg
Electron Distribution Radius	$3\mathring{A}$
Ion Distribution Radius	$3\mathring{A}$
Inter-Atomic Distance IAD	$10\mathring{A}$
Initial Particle Kinetic Energy K_0	0
Light Intensity I	10^{10} W/cm^2
Light Frequency ω_0	$3.75 * 10^{14}$ s^{-1}
Light Pulse Width	20^{-15} s
Short Range Threshold	$15\mathring{A}$
Time Step δt	$6.5 * 10^{-19}$ s
Grid Spacing δx	$0.1\mathring{A}$
Total Calculation Time	$6.5 * 10^{-13}$ s

3.1 Dipole Chains

To further understand what kind of effects one can expect from dielectric MicPIC calculations it is useful to first look at how simple structures of dipoles interact with a probing light pulse. One such structure is a linear chain of evenly spaced individual scatterers. There are several degrees of freedom in a one dimensional chain such as its orientation with respect to the probing light, the total number of dipoles in the chain and the spacing between each individual scatterer. Before looking into longer chains one can study a system comprising of a single, isolated dipole. The optical response of a single dipole starting at rest and then being forced by a 20 fs pulse is displayed in figure 3.1 and will be used as a point of reference for the results to come.

In figure 3.1 one can see in the frequency response a clear, dominant peak with the same frequency as the incoming light pulse. The first order response is followed by another peak at three times this pulse frequency which is a product of the third order repulsion term (σ) added to the dipole's equations of motion. The expected first and third order responses are not the only features present: the response appears to increase with frequency up until around 9 times the pulse's frequency, with a couple of less pronounces peaks occurring at 5 and 7 times the principle peak. The equation of motion applied to a dipole is similar to that of a simple spring and so there is a fundamental frequency associated to the dipole itself, independent of the driving pulse. The fundamental dipole frequency (ω) used for these calculations is $3.29*10^{15}$ Hz, a value corresponding to nitrogen[4], and it is 8.77 times larger than the driving frequency. The fundamental frequency of the dipoles used explains the peak that appears around 9 times the driving frequency.

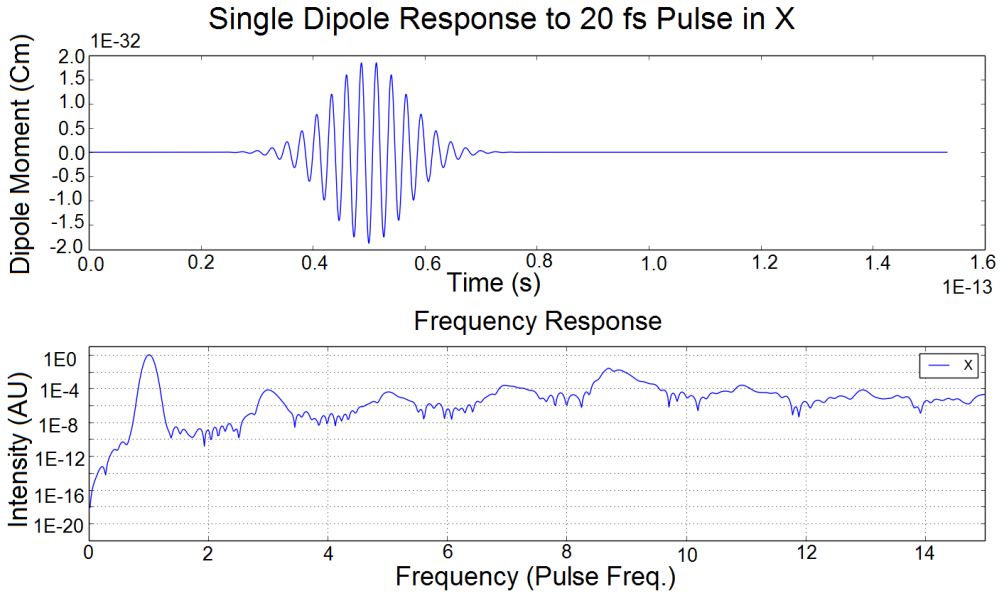

Figure 3.1: Depiction of a single isolated dipole's time and frequency response to an incident light pulse.[10] Arbitrary Units scaled to have the response at driving frequency peak at 1.

One would expect that a single isolated dipole starting from rest would only react to a polarized light source in the same dimension as that light's electric field. Since MicPIC is not an analytic solver there will almost certainly be some along the secondary dimensions due to numerical rounding errors and this is seen in figure 3.2. Tracing the motion profiles of the bound electrons is an intuitive way of understanding their response to the driving field. One can see that the weak response along the propagation dimension (Z) is coherent and not just random noise, a property that is portrayed in figure 3.3. The majority of the Y and Z spectra falls between 6 and 9 orders of magnitude lower than the response in the light's electric field's dimension (X). However, there is a peak at twice the laser frequency that comes within 2 to 3 orders of magnitude of the noise level in X. This unanticipated result at twice the driving frequency is something to look out for when proceeding to larger and more interesting systems of scatterers.

3.1.1 Dipole Pairs

With an established response for a single isolated dipole from the previous section one can begin looking into the effect of dipoles on one another. The simplest of these cases will be when a pair of dipoles are present in the system, interacting with one another and the external field. There are three canonical orientations that will be used for the dipole chains. These orientations have the chain aligned parallel to the electric field (X), the magnetic field (Y) and the propagation direction (Z) of the probing light source.

The first orientation for a dipole pair to consider will have the pair separated along the same dimension as the probing light's magnetic field (Y). In this case each dipole will feel the same external field at the same time as the wave front hits each particle in the chain altogether as shown in fig-

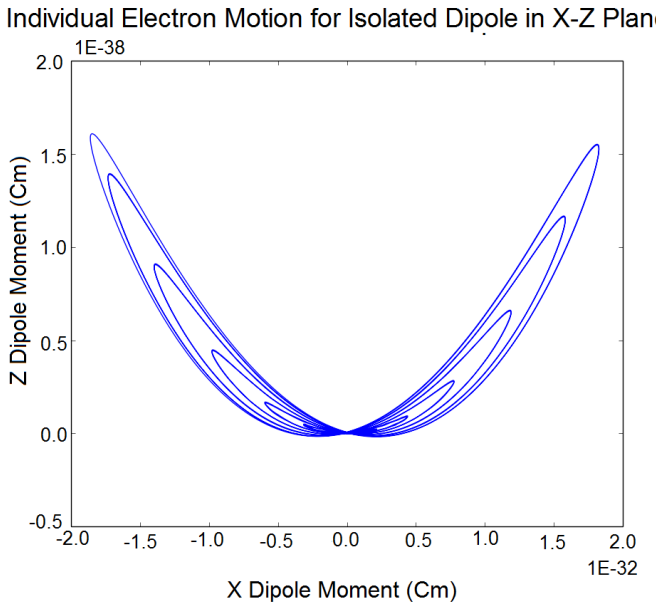

Figure 3.2: Depiction of a single dipole's motion profile traced out in the X-Z plane. The scale for the motion in the Z dimension is 6 orders of magnitude smaller than that of the X motion.[10]

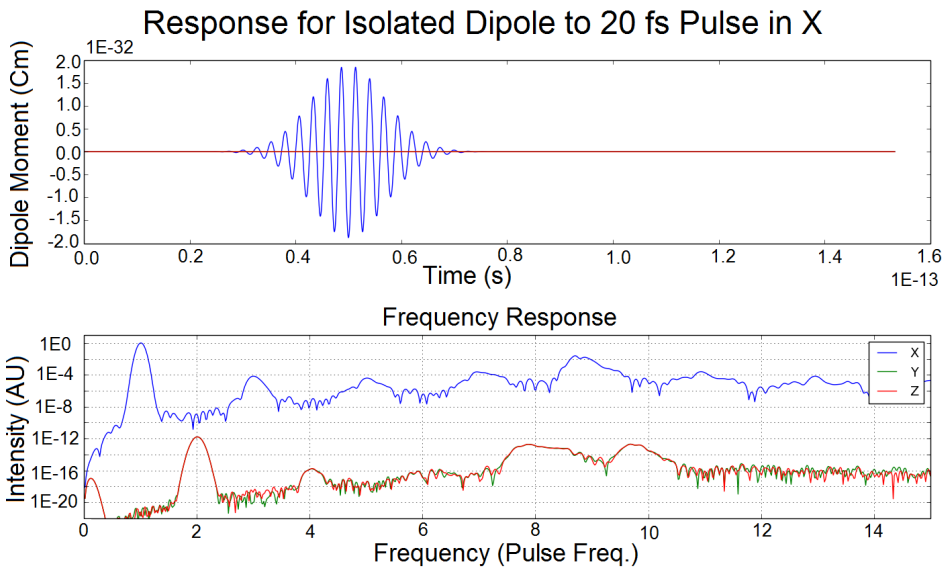

Figure 3.3: Depiction of a single dipole's response parallel to the light's polarization dimension (X), the magnetic field dimension (Y), and the propagation dimension (Z). The secondary Y and Z responses are nearly identical and so cannot be seen easily in this figure.[10]

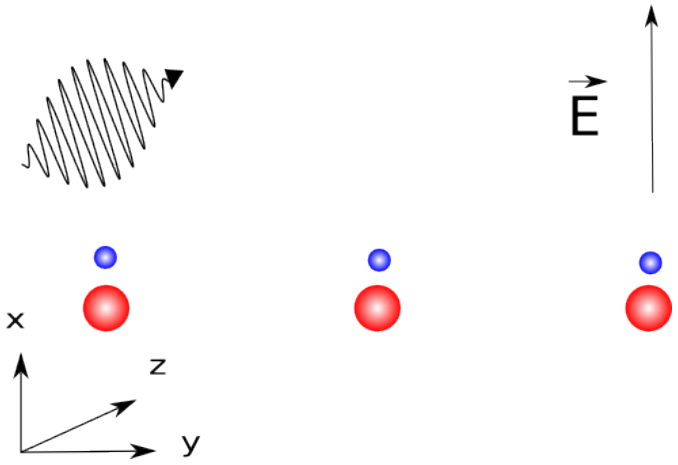

Figure 3.4: Depiction of a chain of dipoles separated along the axis perpendicular to both the propagation direction and the electric field polarization direction of incoming light (Y). Each dipole will experience the same phase of light at the same time.

ure 3.4. The response of a pair of dipoles separated in Y, as compared to an isolated dipole is shown in figure 3.5. Only one of the dipole pairs has been graphed as the two show very similar behavior to one another. One difference between the two is that the response of the isolated dipole at the laser's driving frequency and at three times that frequency is weaker when a neighbour is present. There is a similar decrease in the response at around 9 times the laser frequency, which corresponds to the fundamental frequency of the dipole. This lower response of the dipoles when in each other's presence is opposite to the increase one would get using the Lorentz-Lorentz relation introduced in section 1. Another noteworthy difference is that when separated in Z the dipoles show a peak response at twice the driving frequency which may be tied to the peaks that appear in the secondary dimensions as seen in figure 3.3.

The second orientation of dipole chains that will be explored will be where

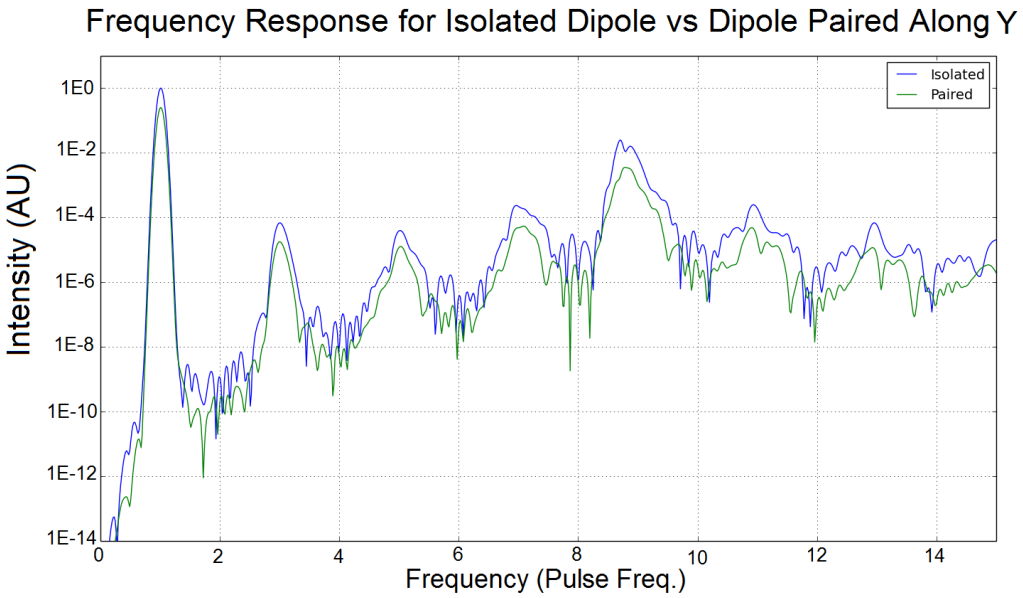

Figure 3.5: Response of isolated dipole versus that of one in a pair 8$\mathring{A}$ apart separated along the Y axis.[10]

the propagation direction of the light pulse is parallel to the chain (Z). As the electric field and propagation direction of a light pulse are perpendicular, the bound electrons will be forced along the electric field's direction perpendicular to the chain's orientation as shown in figure 3.6. In this case the dipoles will experience slightly different phases of the incoming light at a time as the wave front passes through the chain one dipole at a time. Before moving on to longer chains a two dipole system is calculated and one of the two is compared to an isolated dipole as shown in figure 3.7. The peak at twice the light pulse's driving frequency appears for the Z separated pairs and so this trend is not unique to Y.

The final canonical orientation to explore is the one in which dipoles are separated along the electric field axis of the probing light (X). Each dipole will experience the same phase of the light just like in the y orientation, the

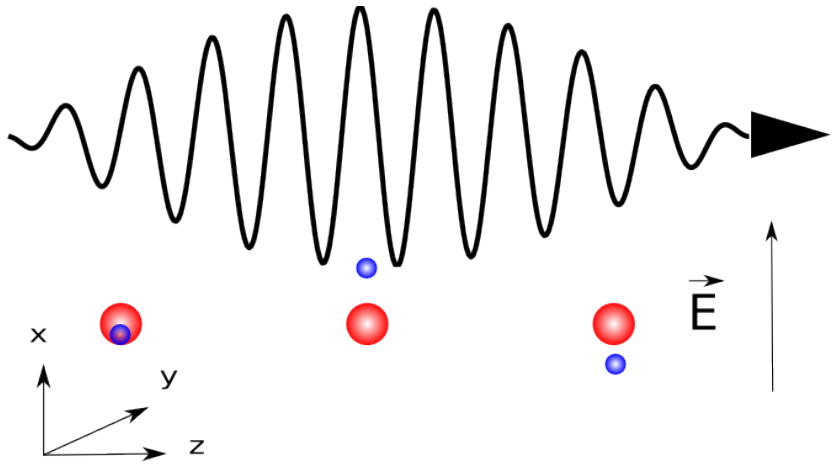

Figure 3.6: Depiction of a chain of dipoles separated along the same direction as the incoming light is traveling. Each dipole will experience a different phase of light based on its location along the chain.

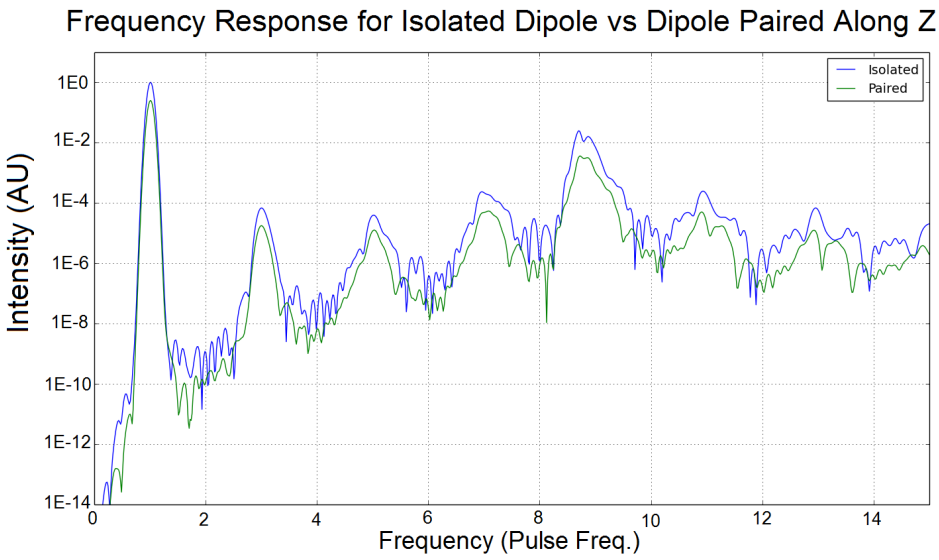

Figure 3.7: Response of isolated dipole versus that of one in a pair $8\mathring{A}$ apart separated along the z axis.[10]

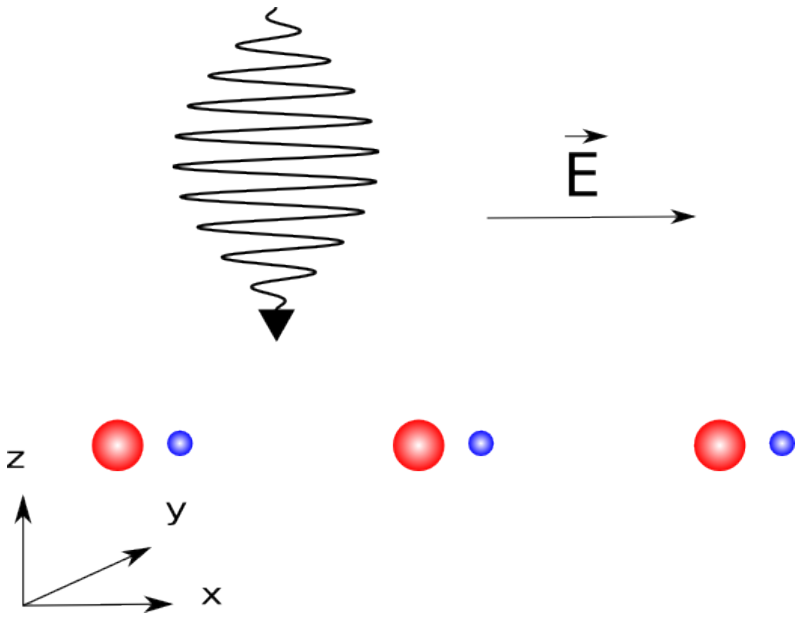

Figure 3.8: Depiction of a chain of dipoles separated in the same direction as their polarization. Each dipole will experience the same phase of light at the same time.

difference being that the external field will force the bound electrons to move directly towards or away from the dipole's neighbours as shown in figure 3.8. By forcing bound electrons to move closer to other dipoles they will feel a stronger effect from the neighbouring scatterer and some interesting phenomena are found. A pair of X separated dipoles is compared to the single dipole system in figure 3.9. One can see a peak at twice the light frequency appears in this orientation as well and that the direct response to the light pulse is again lower when the system comprises of multiple dipoles.

3.1.2 Extended Dipole Chains

Extending beyond a system of two dipoles one introduces boundaries where the outmost dipoles may respond differently to the dipoles in the center of

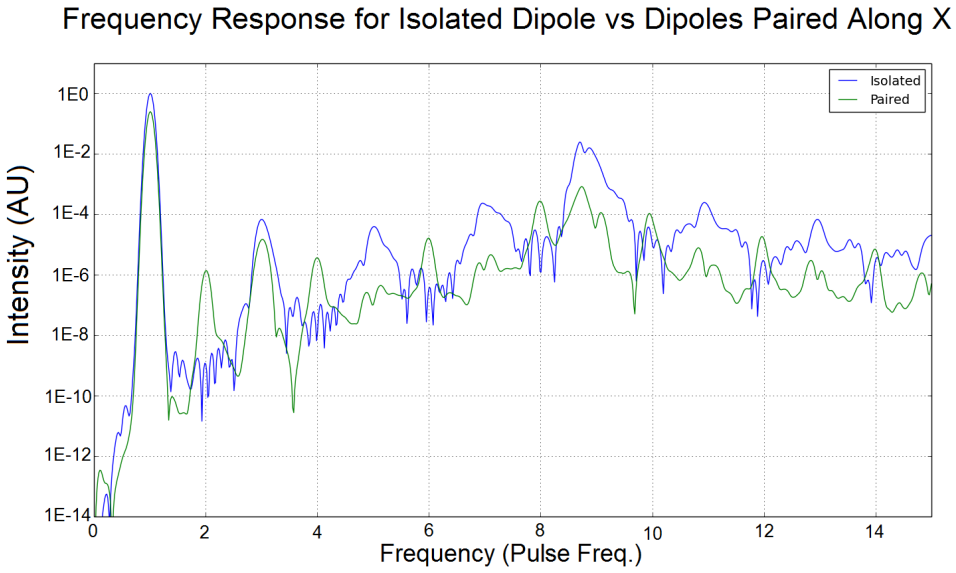

Figure 3.9: Response of isolated dipole versus that of one in a pair $8\mathring{A}$ apart separated along the x axis.[10]

the chain. [4] When a dipole is located in the middle of a long chain of similarly acting dipoles there will be particle-particle interactions coming from each other dipole in the chain. Some of the farther dipoles will have insignificant effects because the dipole force falls off as $1/r^3$, [4] meaning one could get nearly the same response from the central dipole even if the effect from extreme dipoles were ignored. If the influence of one dipole on another is only significant over a short distance then dipoles beyond this threshold distance could effectively be ignored. With a maximum range for particle-particle interactions some of the central dipoles, in a regular chain with uniform polarizations, will experience equal forces from their neighbours on either side. Figure 3.10 shows a chain where each dipole will only have a significant effect on 2 of its neighbours. In the chain of 7 the three central dipoles have the same number of significant neighbours on either end. Since

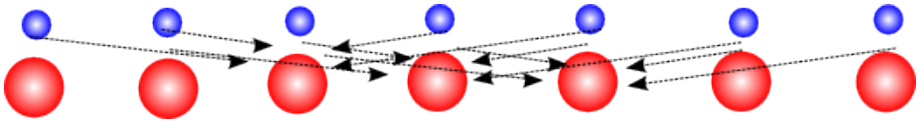

Figure 3.10: Depiction of a chain of equally spaced dipoles. Each of the three internal dipoles is acted on by its neighbours in a similar fashion. The force applied on all of the central dipoles will be similar as long as there are the same number of dipoles on either side that are close enough to have a significant effect.

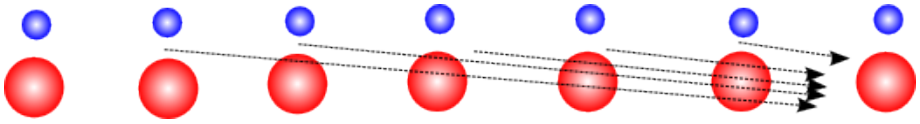

Figure 3.11: Depiction of the boundary of a chain of equally spaced dipoles. The far right dipole experiences forces from neighbours only on one side. This different application of forces as compared to the non-boundary dipoles shown in figure 3.10 will result in a different response when close to the boundary.

those neighbours are acting in a uniform fashion one can see that each of the central dipoles will experience the same effects from the rest of the chain. These central dipoles are not considered be a part of the chain's boundary.

The dipoles located at either extreme of a chain will experience different effects from the rest of the chain as compared to non-boundary dipoles. As displayed in figure 3.11 the right most dipole will experience particle-particle interactions from the inside of the chain, but nothing from the other side as there are no dipoles out there. This shows why one would expect so see different responses from dipoles at each extreme of a chain as compared to the inner dipoles.

The first extended chain to display will be a chain of 48 dipoles separated

along the light's magnetic field (Y). The frequency response of the first 4 dipoles is displayed in figure 3.12. There is little difference to the responses based on position along the chain that can not be attributed to noise. The similarities between the dipoles along the chain extends beyond 4 dipoles; however, only 4 were charted to keep figure 3.12 legible. The consistence of the dipole reactions is sensible for this orientation of dipoles as each one will experience the exact same external force from the light pulse at the same time. Having a consistent response along a dimension can be useful in reducing computation time for two and three dimensional calculations. By placing periodic boundaries at each extreme of the Y dimension, which allow fields to pass out of one end of the domain and into the other, the system will behave as though it is immediately next to another copy of itself in each Y direction. As field values are free to pass through the periodic boundary multiple times the system acts as though it is a small section of an infinitely long domain, which will be useful when calculating periodic macroscopic assortments of particles. This result shows that the Y dimension is a good candidate for periodic boundary conditions when running larger multi-dimensional calculations.

The next extended chain to look into is one of 48 dipoles, this time separated along Z. Again the first 4 dipole responses are displayed for legibility in figure 3.13 as the rest have a similar response. The even harmonics are clear and present for each dipole in the system, as was the case for the Z separated pair of dipoles. Having a response that is independent of location in a Z separated chain is not what one might immediately expect, given different dipoles will experience different phases of light. The 48 dipole long chain, however, only has a physical length of $480\mathring{A}$ as the dipoles are only $10\mathring{A}$ apart. Using a light pulse of infrared radiation with $8000\mathring{A}$ wavelength,

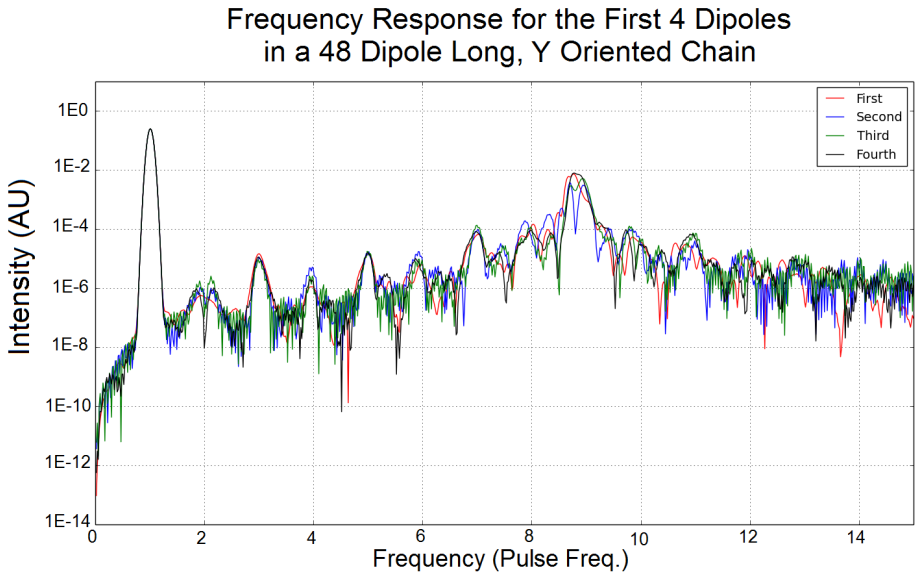

Figure 3.12: Response of the first six dipoles in a chain of 48 separated along Y by 10$\mathring{A}$.[10]

as is done in these calculations, the total chain length is just over 5 % of the light's wavelength. Longer chains are needed in order to see effects at the wavelength's scale.

Finally the dipole pair separated along the X dimension is also extended to a chain 48 long and the first 4 frequency responses are displayed in figure 3.14. The first thing to note is that the variance between dipoles is much greater in this case than it was for the other chain orientations in figures 3.12 and 3.13. Since the light's electric field is driving the bound electrons directly towards and away from the neighbouring dipoles there appears to be much more interaction between the dipoles. Another thing to note is that boundary effects are visible as the first two dipoles from the edge of the chain have a much higher response at twice of the driving frequency. The effect of the boundary on this second order response is shown more clearly in figure

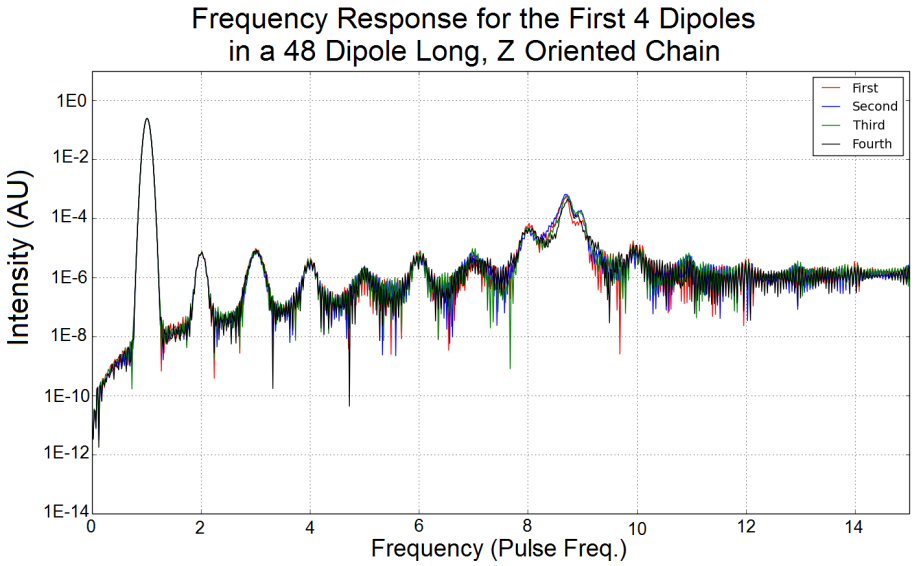

Figure 3.13: Response of the first six dipoles in a chain of 48 separated along Z by 10$\mathring{A}$.[10]

3.15. Here the second order response is plotted against the position of the dipole along the chain and the dependence of the response on position is clearly shown to be much stronger when much closer to either edge.

The trend of having the first two dipoles on either end reacting more strongly at twice the laser frequency starts to appear long before the chain becomes 48 dipoles in length. In figure 3.16 the responses of the first four dipoles of many different length chains are shown and the first two on either end follow the same pattern regardless of the number of remaining internal dipoles. The only apparent outlier that appears is the chain of 4 dipoles in which the boundary effect from the far side of the chain is visible.

One can look at the average of each dipole's response within one of the chains and see how it compares to an isolated dipole. This comparison of the single dipole to the average is shown in figures 3.17, 3.18 and 3.19 for X Y

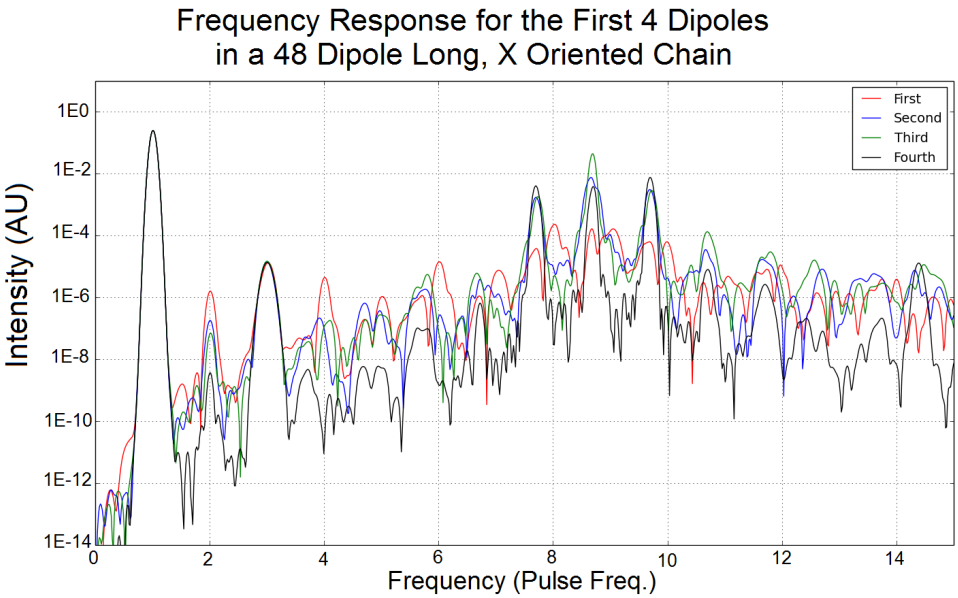

Figure 3.14: Response of the first six dipoles in a chain of 48 separated along the light's electric field polarization dimension (X) by $10\mathring{A}$. There is more variance in the response of the dipoles at higher frequencies than in the Y and Z dimensions. The first and second dipoles from the end have significantly higher responses at twice the driving frequency.[10]

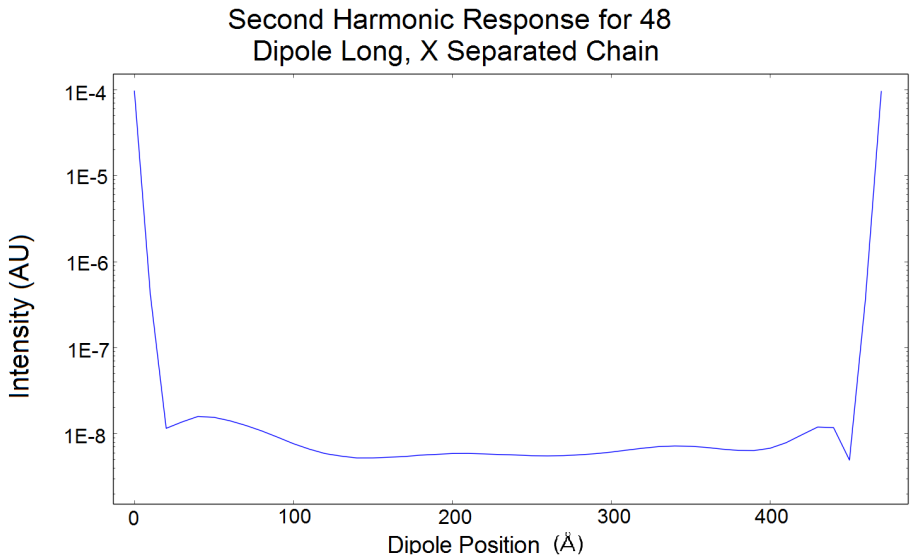

Figure 3.15: Response at twice the driving light frequency of dipoles in a chain of 48 separated along X by 10$\mathring{A}$. The extreme dipoles from each end have significantly higher responses than the central dipoles.[10]

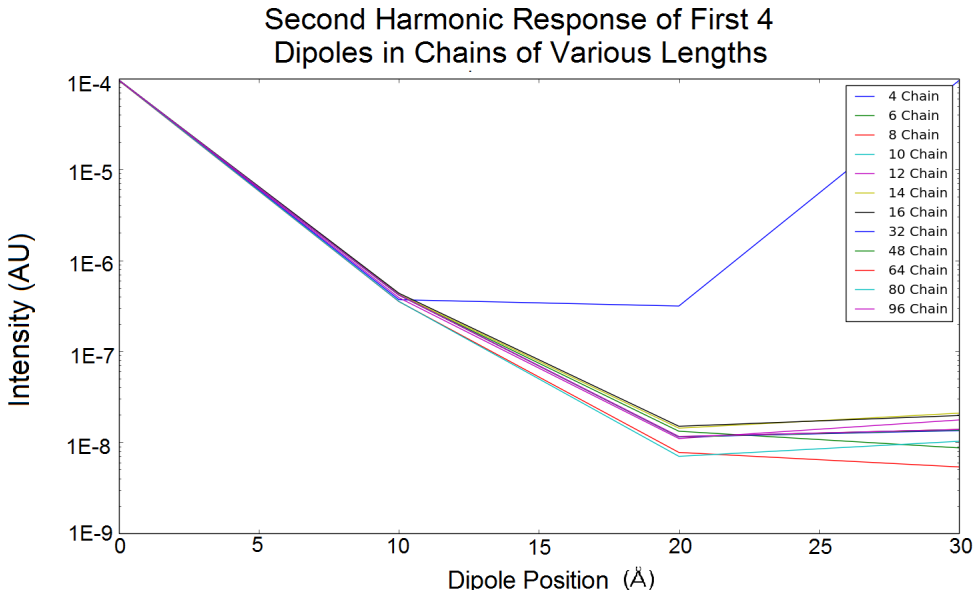

Figure 3.16: Response at twice the driving light frequency of the first 4 dipoles in chains of various lengths along X and each dipole is separated by $10\mathring{A}$. The trend of having two dipoles with stronger responses at the extremes is apparent regardless of the chain length.[10]

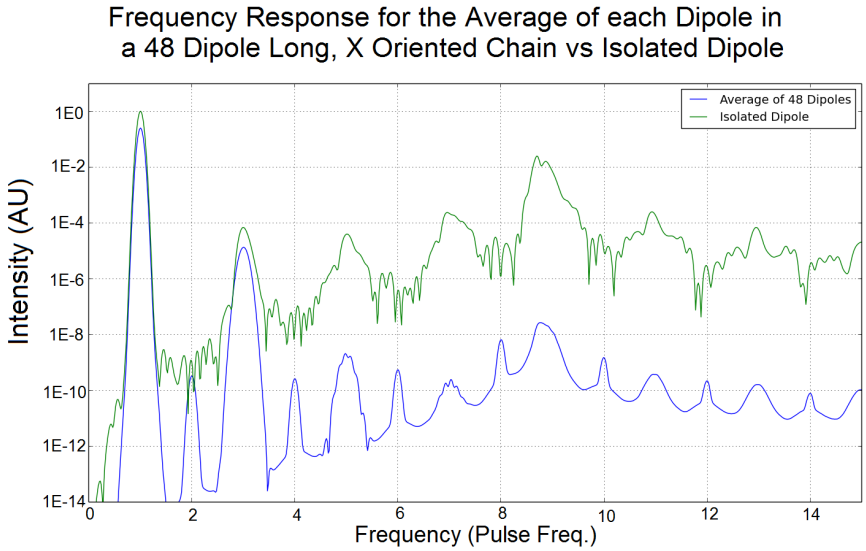

Figure 3.17: Average response of a dipole within a chain of 48 oriented along the light's electric field axis (X) plotted against the response from a single isolated dipole.[10]

and Z oriented chains respectively. The X oriented chain in figure 3.17 shows a much lower average response at high frequencies, due to the uncoordinated response from those dipoles shown in figure 3.14. One general difference to note is that in the chain of dipoles the response at the driving frequency, and the third order response is weaker than that of an isolated dipole. This is the same effect as was seen in section 3.1.1 where the introduction of a second dipole reduced the direct response to the light pulse. This result is again contrary to what would come from using the Lorentz-Lorentz relation from section 1. It is not too surprising that these results do not agree as the MicPIC results are for a one dimensional chain, whereas the Lorentz-Lorentz relation assumes a three dimensional structure of infinite volume in determining the effective local field for each dipole.

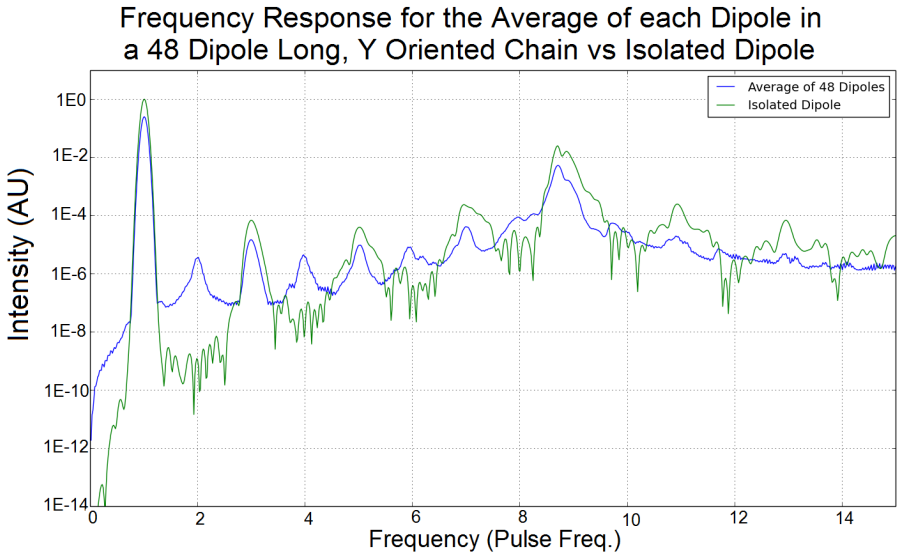

Figure 3.18: Average response of a dipole within a chain of 48 oriented along the light's magnetic field axis (Y) plotted against the response from a single isolated dipole.[10]

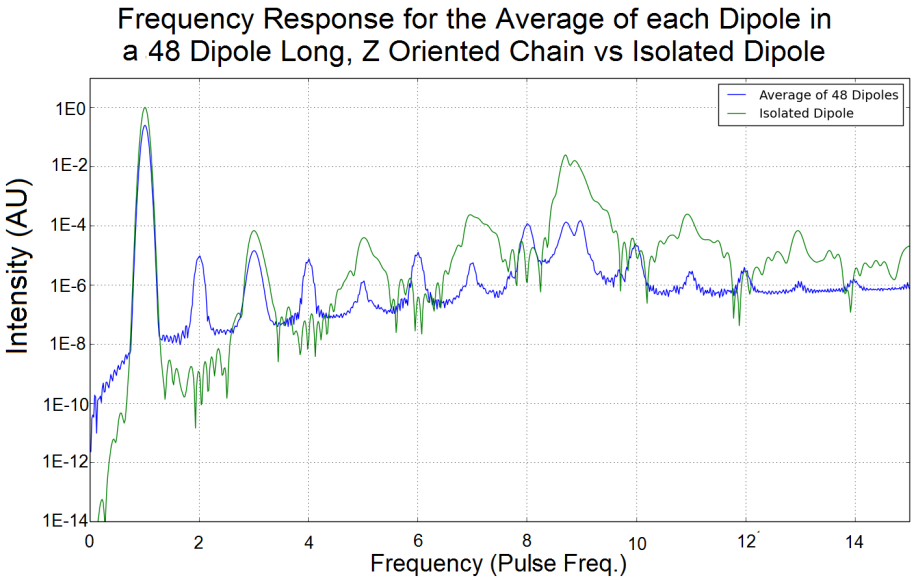

Figure 3.19: Average response of a dipole within a chain of 48 oriented along the light's propagation axis (Z) plotted against the response from a single isolated dipole.[10]

One can see some differences in the average responses of chains of dipoles (figures 3.17, 3.18 and 3.19) based on the orientation of the chain. At twice the driving frequency the average peak for the X oriented chain is much lower than in Y and Z. This is due to the internal dipoles having little to no response at this frequency and so the strong second harmonic generation found in the boundary dipoles is highly diluted in the average. The high variance in the X oriented chain's dipole responses shown in figure 3.14 shows in the average as the Y and Z chains have a constant high frequency noise floor and the X chain shows more high frequency variance.

The orientations of a chain of particles relative to the driving light source have been shown to alter the response of the individual dipoles in the chain. This dependence of a dipole's response on the number and location of its neighbours will be useful in determining which dimensions are worth expanding in three-dimensional calculations. It would be interesting to see if these position dependent characteristics of the dipoles are unique to MicPIC's combination of methods or if they can be produced with strictly electrostatic results.

3.2 Electrostatic Comparisons

The physics of molecular dipole chains can be gained by comparing MicPIC with a pure Molecular Dynamics code. This comparison can distinguish whether the observed phenomena are electromagnetic or electrostatic in nature; for example, the Lorentz Lorentz relation shown in section 1 is derived by electrostatic arguments. Similarly to MicPIC, in an MD code particles are represented as objects with a certain position in the domain and they interact directly via the Coulomb force (equation 1.11) with other particles.

The electrostatic results used to compare with MicPIC were taken using a Molecular Dynamics code created by Lucien Deveau.[12] The first comparison to make is that of a single isolated dipole's response calculated with each technique (figure 3.20). One can see that there is an agreement at the three principle peaks (first order light frequency, third order light frequency and the dipole's fundamental frequency) but elsewhere there is a high noise floor for the MicPIC results. This result is partially expected as there are more opportunities in MicPIC for numerical errors to compound than there are without an FDTD grid for the dipole to interact with. A separate calculation in MicPIC ignoring the influence of the generated field is compared to the electrostatic results in figure 3.21. The noise floor is seen to reduce drastically when field effects are removed, giving a clear indicator as to the origin of the high frequency noise present in other MicPIC results. The comparison with the electrostatic results lines up well at 1, 3 and 9 times the pulse frequency everywhere except around the dipole's fundamental frequency, which appears around 9 times the pulse frequency. It is not clear at this time what the source of this discrepancy is and future work will be needed to determine it.

When extending to a system to more than a single dipole the presence of a neighbour does not influence the individual responses nearly as much as was the case for MicPIC in section 3.1. Figure 3.22 shows the evolution of one of a pair of dipoles against the isolated case from figures 3.20 and 3.21. The two dipole motion profiles are practically identical as compared to the more drastic difference when a neighbour was introduced in figure 3.9. This trend of individual dipoles not being as significantly affected by the presence of the rest of the chain extends beyond dipole pairs and the difference from one dipole to the next for a chain of 64 is shown in figure 3.23. Here one

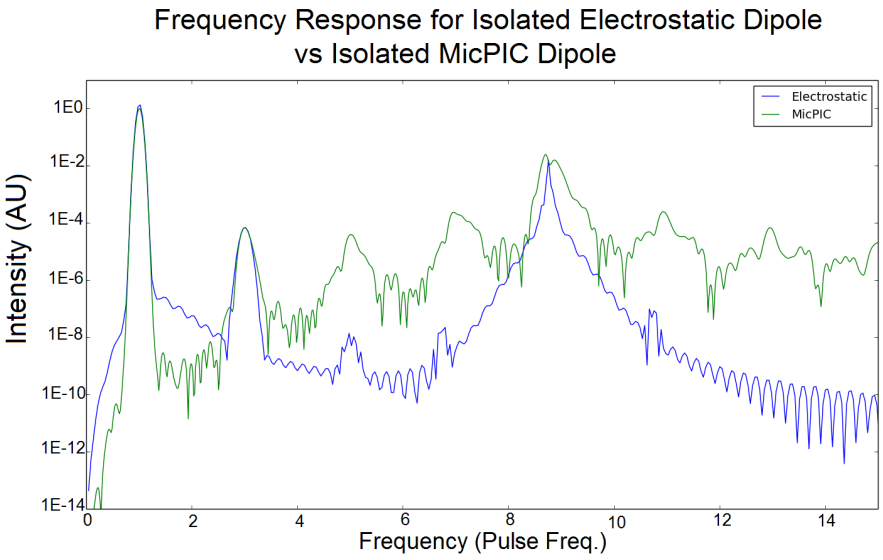

Figure 3.20: Comparison of a single isolated dipole's response calculated by MicPIC versus the same dipole response calculated solely electro-statically. The response lines up at the light pulse's frequency, the third order frequency and the dipole resonant frequency. There is a higher noise floor for the MicPIC calculation at higher frequencies that is not present in the electrostatic calculation.[10]

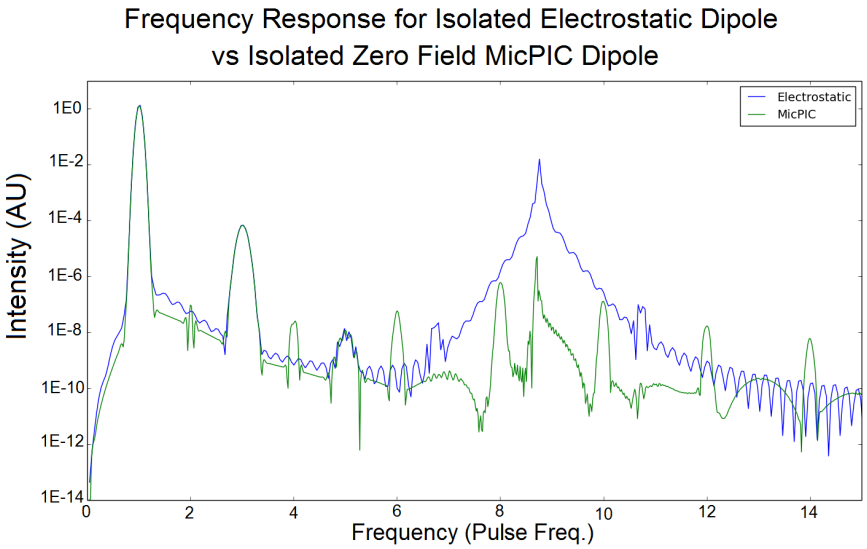

Figure 3.21: Comparison of a single isolated dipole's response calculated by MicPIC without any influence from the field created from the dipole versus the same dipole with response calculated solely electro-statically. The noise floor has been reduced greatly and the two sets of dipole responses agree everywhere except at the dipole's fundamental frequency. This in combination with figure 3.20 shows that the noise floor is a product of the field generated by the dipole.[10]

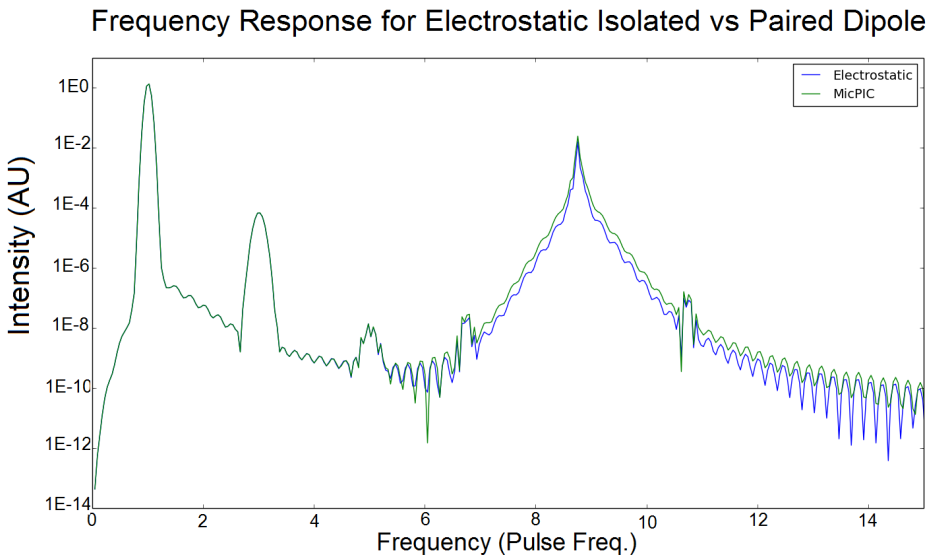

Figure 3.22: Response of an isolated dipole compared to one in a paired system of dipoles.[10]

can only see a couple of the individual dipole responses as they are all nearly identical. Given these electrostatic results, the even harmonic generation seen in section 3.1 for boundary dipoles seems to be an electrodynamic effect caused by the Particle-in-Cell part of MicPIC, since it does not appear in the strictly electrostatic results at all.

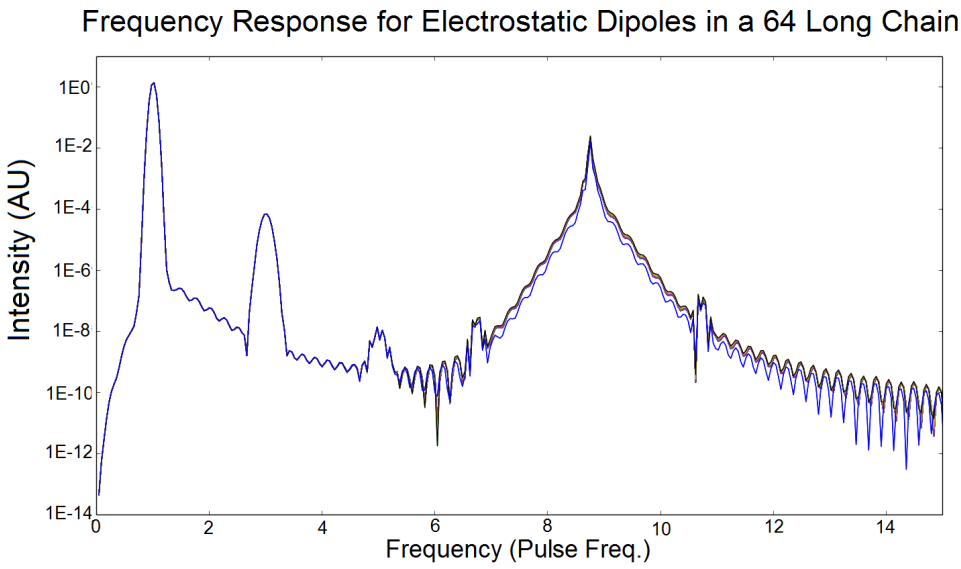

Figure 3.23: Response of 64 dipoles in a chain calculated electro-statically. The responses are so nearly independent of one another that it is difficult to see each one individually as they are all overlaid on top of one another.[10]

4

Conclusion

In order to study non-linear optics in the atomic limit a wide range of scales is needed if one is looking for macroscopic results. By studying how the response of systems evolve with increasing domain sizes one can determine ways of reducing the computational cost while losing only minimal accuracy in the results. The Microscopic Particle-In-Cell technique is one such tool that can be used to accurately calculate short range interactions between particles while keeping low computational cost for long range electrodynamic calculations. The hybrid technique allows for the response of light matter interactions in a wide range of scales and so reducing its cost would allow for highly accurate calculations of larger macroscopic arrangements of particles.

The results displayed in section 3.1.1 showed that the presence of another dipole altered the response of its neighbours. A decreased response at the light pulse's frequency and a small second harmonic generation appear in dipoles when introduced to a neighbour. The dipoles being close enough to have a significant impact on one another is something that would be lost in calculations using volume approximations such as the Lorentz-Lorentz relation.

In section 3.1.2 it was shown that in 1D chains of dipoles extension along the same dimension as light's electric field is polarized (X) there was a second harmonic generated only in the boundary dipoles of the chain. Having the chain oriented along either the light's magnetic field (Y), or propagation (Z) dimension gave little variance in the dipoles' responses. If this symmetry extends to 3 dimensional structures one could reduce the domain size along this dimension to a small number of dipoles and apply periodic boundaries, saving processing power for the more interesting variances in other dimensions.

There is plenty of opportunity to expand what can be done in computational physics. MicPIC allows one to study light-matter interactions in the atomic limit for highly resolved results. With proper study of how these atomic scale interactions vary with scale MicPIC can be used to cover a wide range of light-matter interactions.

References

[1] Hugh D. Young *University Physics* Pearson Education 12th Edition, 2006.

[2] Fowles, Grant *Introduction to Modern Optics*. New York: Dover Publications. 1975.

[3] Press, William H. *Numerical Recipes: The Art of Scientific Computing* Cambridge University Press, 2007.

[4] Boyd, Robert *Nonlinear Optics*. Burlington: Academic Press. 3rd Edition, 2008.

[5] DeVoe H. *Optical properties of molecular aggregates. I. Classical model of electronic absorption and refraction* Volume 41, Page 393 J. Chem. Phys. 1964.

[6] Varin, Charles *Attosecond Plasma Wave Dynamics in Laser-Driven Cluster Nanoplasmas* Physics Review Letters. Volume 108, Issue 17 2012.

[7] Jackson, John *Classical Electrodynamics*. Berkeley: John Wiley & Sons, Inc. 3rd Edition, 1999.

[8] Humphrey, William *VMD: Visual Molecular Dynamics* Journal of Molecular Graphics. Volume 14, Issue 1, 1996.

[9] Peltz, Christian *Fully microscopic analysis of laser-driven finite plasmas using the example of clusters* New Journal of Physics. Volume 14, 2012.

[10] Hunter, J. D. *Matplotlib: A 2D graphics environment* IEEE COMPUTER SOC. 2007.

[11] Daniel, Jacob *Introduction to Atmospheric Chemistry* Princeton University Press. 1999.

[12] Deveau, Lucien *Theoretical Analysis of Microscopic Electrostatic Nonlinear Optics in Simple Structures* University of Ottawa. 2016.